11

Shear Strength of Soil

The *shear strength* of a soil mass is the internal resistance per unit area that the soil mass can offer to resist failure and sliding along any plane inside it. One must understand the nature of shearing resistance in order to analyze soil stability problems such as bearing capacity, slope stability, and lateral pressure on earthretaining structures.

11.1 Mohr–Coulomb Failure Criterion

Mohr (1900) presented a theory for rupture in materials that contended that a material fails because of a critical combination of normal stress and shearing stress, and not from either maximum normal or shear stress alone. Thus, the functional relationship between normal stress and shear stress on a failure plane can be expressed in the following form:

$$\tau_f = f(\sigma) \tag{11.1}$$

The failure envelope defined by Eq. (11.1) is a curved line. For most soil mechanics problems, it is sufficient to approximate the shear stress on the failure plane as a linear function of the normal stress (Coulomb, 1776). This linear function can be written as

$$\tau_f = c + \sigma \tan \phi \tag{11.2}$$

where c = cohesion
ϕ = angle of internal friction
σ = normal stress on the failure plane
τ_f = shear strength

The preceding equation is called the *Mohr–Coulomb failure criterion.*

In saturated soil, the total normal stress at a point is the sum of the effective stress (σ') and pore water pressure (u), or

$$\sigma = \sigma' + u$$

Table 11.1 Typical Values of Drained Angle of Friction for Sands and Silts

Soil type	ϕ' (deg)
Sand: Rounded grains	
Loose	27–30
Medium	30–35
Dense	35–38
Sand: Angular grains	
Loose	30–35
Medium	35–40
Dense	40–45
Gravel with some sand	34–48
Silts	26–35

The effective stress σ' is carried by the soil solids. The Mohr–Coulomb failure criterion, expressed in terms of effective stress, will be of the form

$$\tau_f = c' + \sigma' \tan \phi' \tag{11.3}$$

where c' = cohesion and ϕ' = friction angle, based on effective stress.

Thus, Eqs. (11.2) and (11.3) are expressions of shear strength based on total stress and effective stress. The value of c' for sand and inorganic silt is 0. For normally consolidated clays, c' can be approximated at 0. Overconsolidated clays have values of c' that are greater than 0. The angle of friction, ϕ', is sometimes referred to as the *drained angle of friction.* Typical values of ϕ' for some granular soils are given in Table 11.1.

The significance of Eq. (11.3) can be explained by referring to Fig. 11.1, which shows an elemental soil mass. Let the effective normal stress and the shear stress on

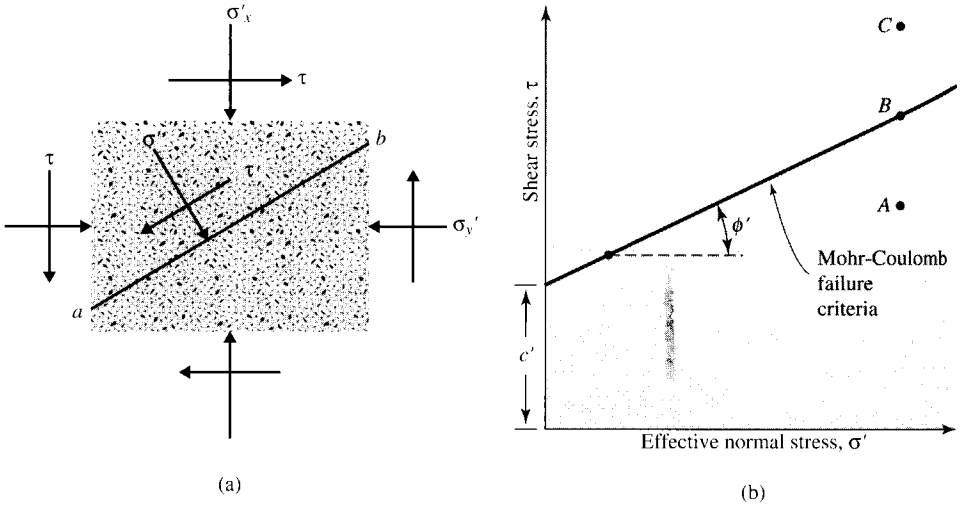

Figure 11.1 Mohr–Coulomb failure criterion

the plane ab be σ' and τ, respectively. Figure 11.1b shows the plot of the failure envelope defined by Eq. (11.3). If the magnitudes of σ' and τ on plane ab are such that they plot as point A in Figure 11.1b, shear failure will not occur along the plane. If the effective normal stress and the shear stress on plane ab plot as point B (which falls on the failure envelope), shear failure will occur along that plane. A state of stress on a plane represented by point C cannot exist, because it plots above the failure envelope, and shear failure in a soil would have occurred already.

11.2 Inclination of the Plane of Failure Caused by Shear

As stated by the Mohr–Coulomb failure criterion, failure from shear will occur when the shear stress on a plane reaches a value given by Eq. (11.3). To determine the inclination of the failure plane with the major principal plane, refer to Figure 11.2, where σ'_1 and σ'_3 are, respectively, the major and minor effective principal stresses. The failure plane EF makes an angle θ with the major principal plane. To determine the angle θ and the relationship between σ'_1 and σ'_3, refer to Figure 11.3, which is a plot of the Mohr's circle for the state of stress shown in Figure 11.2 (see Chapter 9). In Figure 11.3, fgh is the failure envelope defined by the relationship $\tau_f = c' + \sigma' \tan \phi'$. The radial line ab defines the major principal plane (CD in Figure 11.2), and the radial line ad defines the failure plane (EF in Figure 11.2). It can be shown that $\angle bad = 2\theta = 90 + \phi'$, or

$$\theta = 45 + \frac{\phi'}{2} \tag{11.4}$$

Again, from Figure 11.3,

$$\frac{\overline{ad}}{\overline{fa}} = \sin \phi' \tag{11.5}$$

$$\overline{fa} = fO + Oa = c' \cot \phi' + \frac{\sigma'_1 + \sigma'_3}{2} \tag{11.6a}$$

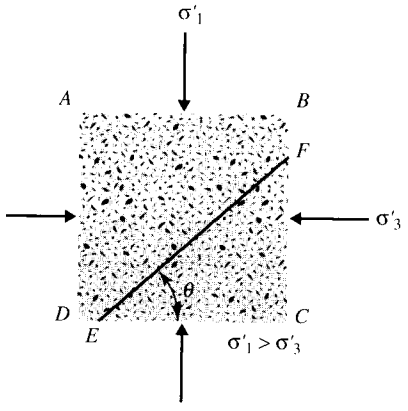

Figure 11.2 Inclination of failure plane in soil with major principal plane

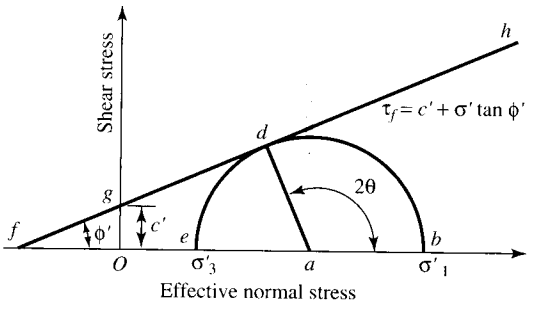

Figure 11.3 Mohr's circle and failure envelope

Also,

$$\overline{ad} = \frac{\sigma_1' - \sigma_3'}{2} \tag{11.6b}$$

Substituting Eqs. (11.6a) and (11.6b) into Eq. (11.5), we obtain

$$\sin \phi' = \frac{\dfrac{\sigma_1' - \sigma_3'}{2}}{c' \cot \phi' + \dfrac{\sigma_1' + \sigma_3'}{2}}$$

or

$$\sigma_1' = \sigma_3'\left(\frac{1 + \sin \phi'}{1 - \sin \phi'}\right) + 2c\left(\frac{\cos \phi'}{1 - \sin \phi'}\right) \tag{11.7}$$

However,

$$\frac{1 + \sin \phi'}{1 - \sin \phi'} = \tan^2\left(45 + \frac{\phi'}{2}\right)$$

and

$$\frac{\cos \phi'}{1 - \sin \phi'} = \tan\left(45 + \frac{\phi'}{2}\right)$$

Thus,

$$\sigma_1' = \sigma_3' \tan^2\left(45 + \frac{\phi'}{2}\right) + 2c' \tan\left(45 + \frac{\phi'}{2}\right) \tag{11.8}$$

An expression similar to Eq. (11.8) could also be derived using Eq. (11.2) (that is, total stress parameters c and ϕ), or

$$\sigma_1 = \sigma_3 \tan^2\left(45 + \frac{\phi}{2}\right) + 2c \tan\left(45 + \frac{\phi}{2}\right) \tag{11.9}$$

11.3 Laboratory Test for Determination of Shear Strength Parameters

There are several laboratory methods now available to determine the shear strength parameters (i.e., c, ϕ, c', ϕ') of various soil specimens in the laboratory. They are as follows:

a. Direct shear test
b. Triaxial test
c. Direct simple shear test
d. Plane strain triaxial test
e. Torsional ring shear test

The direct shear test and the triaxial test are the two commonly used techniques for determining the shear strength parameters. These two tests will be described in detail in the sections that follow.

11.4 Direct Shear Test

The direct shear test is the oldest and simplest form of shear test arrangement. A diagram of the direct shear test apparatus is shown in Figure 11.4. The test equipment consists of a metal shear box in which the soil specimen is placed. The soil specimens may be square or circular in plan. The size of the specimens generally used is about 51 mm × 51 mm or 102 mm × 102 mm (2 in. × 2 in. or 4 in. × 4 in.) across and about 25 mm (1 in.) high. The box is split horizontally into halves. Normal force on the specimen is applied from the top of the shear box. The normal stress on the specimens can be as great as 1050 kN/m^2 (150 lb/in.^{2}). Shear force is applied by moving one-half of the box relative to the other to cause failure in the soil specimen.

Depending on the equipment, the shear test can be either stress controlled or strain controlled. In stress-controlled tests, the shear force is applied in equal increments until the specimen fails. The failure occurs along the plane of split of the shear box. After the application of each incremental load, the shear displacement of the top half of the box is measured by a horizontal dial gauge. The change in the height of the specimen (and thus the volume change of the specimen) during the test can be obtained from the readings of a dial gauge that measures the vertical movement of the upper loading plate.

In strain-controlled tests, a constant rate of shear displacement is applied to one-half of the box by a motor that acts through gears. The constant rate of shear displacement is measured by a horizontal dial gauge. The resisting shear force of the soil corresponding to any shear displacement can be measured by a horizontal proving ring or load cell. The volume change of the specimen during the test is obtained

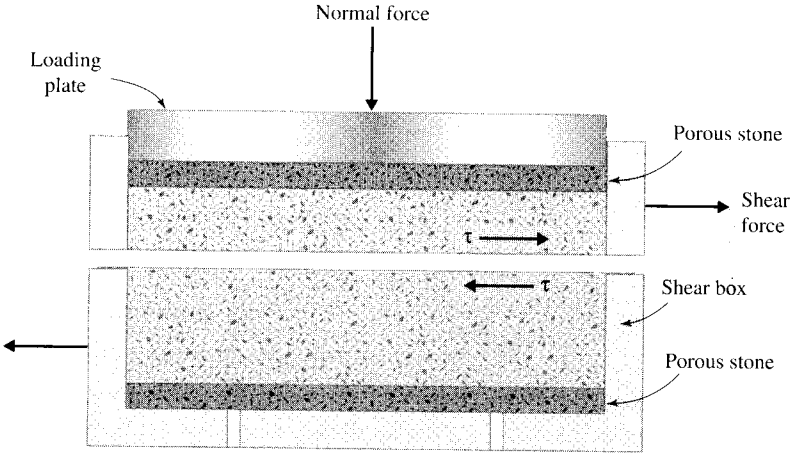

Figure 11.4 Diagram of direct shear test arrangement

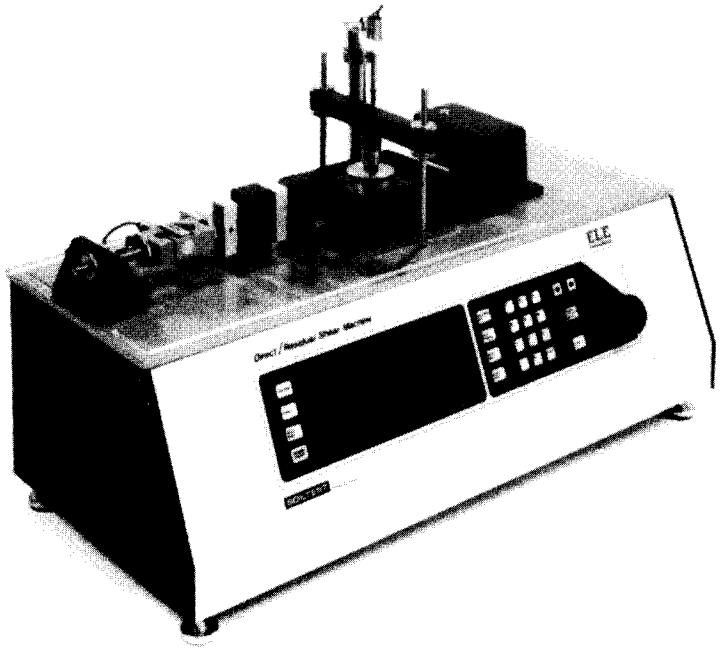

Figure 11.5 Strain-controlled direct shear test equipment (courtesy of Soiltest, Inc., Lake Bluff, Illinois)

in a manner similar to that in the stress-controlled tests. Figure 11.5 shows a photograph of strain-controlled direct shear test equipment.

The advantage of the strain-controlled tests is that in the case of dense sand, peak shear resistance (that is, at failure) as well as lesser shear resistance (that is, at a point after failure called *ultimate strength*) can be observed and plotted. In stress-controlled tests, only the peak shear resistance can be observed and plotted. Note that the peak shear resistance in stress-controlled tests can be only approximated because failure occurs at a stress level somewhere between the prefailure load increment and the failure load increment. Nevertheless, compared with strain-controlled tests, stress-controlled tests probably model real field situations better.

For a given test, the normal stress can be calculated as

$$\sigma = \text{Normal stress} = \frac{\text{Normal force}}{\text{Cross-sectional area of the specimen}} \tag{11.10}$$

The resisting shear stress for any shear displacement can be calculated as

$$\tau = \text{Shear stress} = \frac{\text{Resisting shear force}}{\text{Cross-sectional area of the specimen}} \tag{11.11}$$

Figure 11.6 shows a typical plot of shear stress and change in the height of the specimen against shear displacement for dry loose and dense sands. These observations were obtained from a strain-controlled test. The following generalizations can

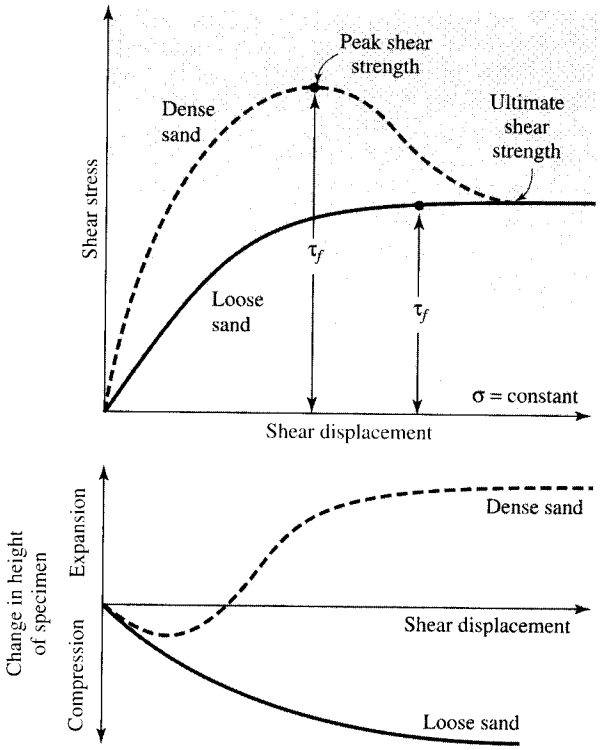

Figure 11.6 Plot of shear stress and change in height of specimen against shear displacement for loose and dense dry sand (direct shear test)

be developed from Figure 11.6 regarding the variation of resisting shear stress with shear displacement:

1. In loose sand, the resisting shear stress increases with shear displacement until a failure shear stress of τ_f is reached. After that, the shear resistance remains approximately constant for any further increase in the shear displacement.
2. In dense sand, the resisting shear stress increases with shear displacement until it reaches a failure stress of τ_f. This τ_f is called the *peak shear strength.* After failure stress is attained, the resisting shear stress gradually decreases as shear displacement increases until it finally reaches a constant value called the *ultimate shear strength.*

It is important to note that, in dry sand,

$$\sigma = \sigma'$$

and

$$c' = 0$$

Direct shear tests are repeated on similar specimens at various normal stresses. The normal stresses and the corresponding values of τ_f obtained from a number of tests are plotted on a graph from which the shear strength parameters are determined.

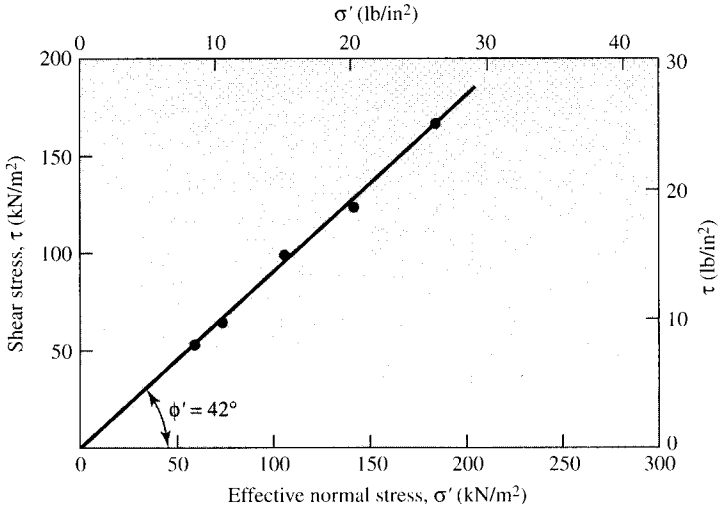

Figure 11.7 Determination of shear strength parameters for a dry sand using the results of direct shear tests

Figure 11.7 shows such a plot for tests on a dry sand. The equation for the average line obtained from experimental results is

$$\tau_f = \sigma' \tan \phi' \tag{11.12}$$

So, the friction angle can be determined as follows:

$$\phi' = \tan^{-1}\left(\frac{\tau_f}{\sigma'}\right)$$

It is important to note that *in situ* cemented sands may show a c' intercept.

11.5 Drained Direct Shear Test on Saturated Sand and Clay

In the direct shear test arrangement, the shear box that contains the soil specimen is generally kept inside a container that can be filled with water to saturate the specimen. A *drained test* is made on a saturated soil specimen by keeping the rate of loading slow enough so that the excess pore water pressure generated in the soil is completely dissipated by drainage. Pore water from the specimen is drained through two porous stones. (See Figure 11.4.)

Because the hydraulic conductivity of sand is high, the excess pore water pressure generated due to loading (normal and shear) is dissipated quickly. Hence, for

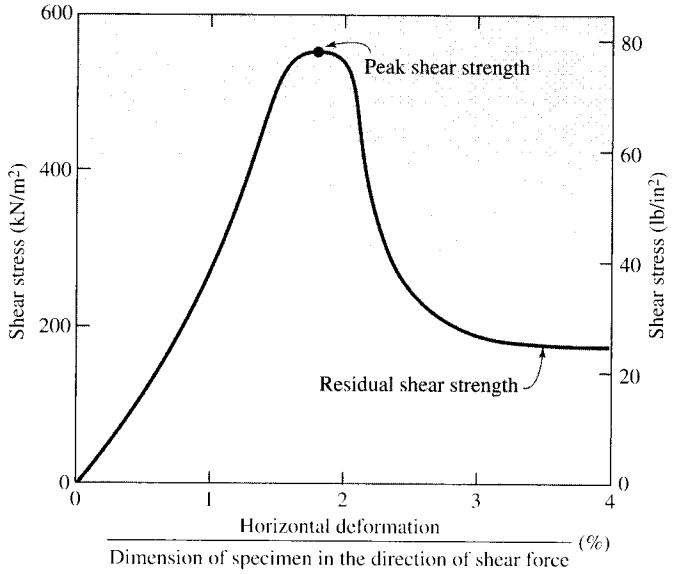

Figure 11.8 Results of a drained direct shear test on an overconsolidated clay. *Note:* Residual shear strength in clay is similar to ultimate shear strength in sand – see Figure 11.6

an ordinary loading rate, essentially full drainage conditions exist. The friction angle, ϕ', obtained from a drained direct shear test of saturated sand will be the same as that for a similar specimen of dry sand.

The hydraulic conductivity of clay is very small compared with that of sand. When a normal load is applied to a clay soil specimen, a sufficient length of time must elapse for full consolidation – that is, for dissipation of excess pore water pressure. For this reason, the shearing load must be applied very slowly. The test may last from two to five days. Figure 11.8 shows the results of a drained direct shear test on an overconsolidated clay. Figure 11.9 shows the plot of τ_f against σ' obtained from a number

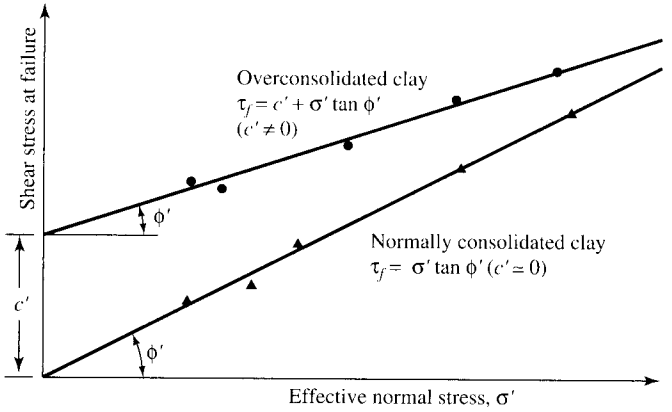

Figure 11.9 Failure envelope for clay obtained from drained direct shear tests

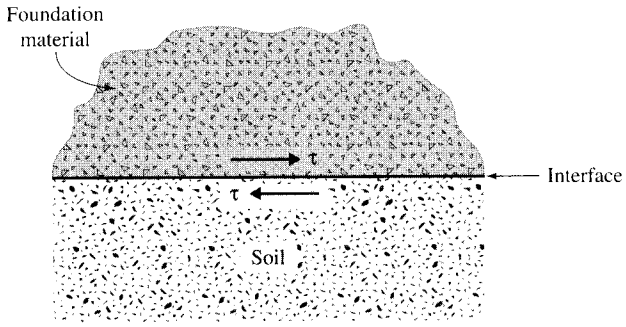

Figure 11.10 Interface of a foundation material and soil

of drained direct shear tests on a normally consolidated clay and an overconsolidated clay. Note that the value of $c' \simeq 0$ for a normally consolidated clay.

11.6 General Comments on Direct Shear Test

The direct shear test is simple to perform, but it has some inherent shortcomings. The reliability of the results may be questioned because the soil is not allowed to fail along the weakest plane but is forced to fail along the plane of split of the shear box. Also, the shear stress distribution over the shear surface of the specimen is not uniform. Despite these shortcomings, the direct shear test is the simplest and most economical for a dry or saturated sandy soil.

In many foundation design problems, one must determine the angle of friction between the soil and the material in which the foundation is constructed (Figure 11.10). The foundation material may be concrete, steel, or wood. The shear strength along the surface of contact of the soil and the foundation can be given as

$$\tau_f = c'_a + \sigma' \tan \delta \tag{11.13}$$

where c'_a = adhesion
δ = effective angle of friction between the soil and the foundation material

Note that the preceding equation is similar in form to Eq. (11.3). The shear strength parameters between a soil and a foundation material can be conveniently determined by a direct shear test. This is a great advantage of the direct shear test. The foundation material can be placed in the bottom part of the direct shear test box and then the soil can be placed above it (that is, in the top part of the box), as shown in Figure 11.11, and the test can be conducted in the usual manner.

Figure 11.12 shows the results of direct shear tests conducted in this manner with a quartz sand and concrete wood, and steel as foundation materials, with $\sigma' =$ 100 kN/m^2 (14.5 lb/in.^{2}).

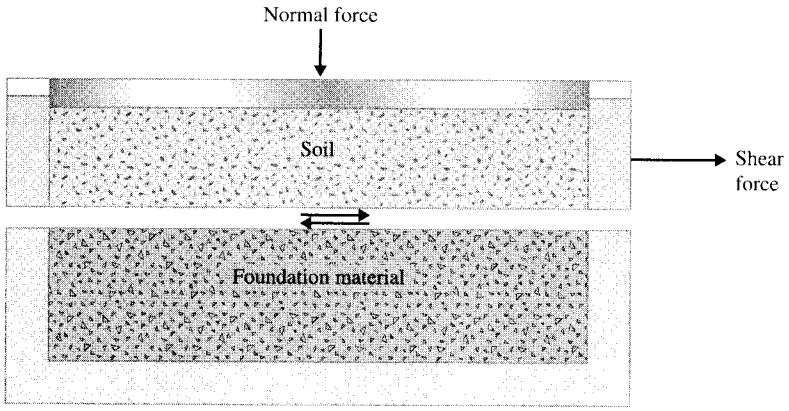

Figure 11.11 Direct shear test to determine interface friction angle

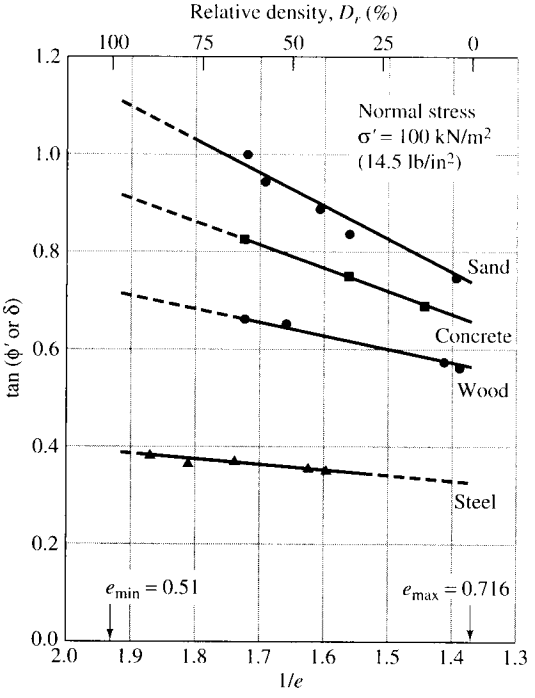

Figure 11.12 Variation of tan ϕ' and tan δ with $1/e$. [*Note:* e = void ratio, $\sigma' = 100$ kN/m^2 (14.5 lb/in.^{2}), quartz sand (after Acar, Durgunoglu, and Tumay, 1982)]

Example 11.1

Following are the results of four drained direct shear tests on an *overconsolidated clay:*

Diameter of specimen = 50 mm

Height of specimen = 25 mm

Test no.	Normal force, N (N)	Shear force at failure, S_{peak} (N)	Residual shear force, $S_{residual}$ (N)[a]
1	150	157.5	44.2
2	250	199.9	56.6
3	350	257.6	102.9
4	550	363.4	144.5

[a] See Figure 11.8

Determine the relationships for *peak shear strength* (τ_f) and *residual shear strength* (τ_r).

Solution

Area of the specimen $(A) = (\pi/4)\left(\frac{50}{1000}\right)^2 = 0.0019634\ \text{m}^2$. Now the following table can be prepared:

Test no.	Normal force, N (N)	Normal stress, σ' (kN/m^2)	Peak shear force, S_{peak} (N)	$\tau_f = \frac{S_{peak}}{A}$ (kN/m^2)	Residual shear force, $S_{residual}$ (N)	$\tau_r = \frac{S_{residual}}{A}$ (kN/m^2)
1	150	76.4	157.5	80.2	44.2	22.5
2	250	127.3	199.9	101.8	56.6	28.8
3	350	178.3	257.6	131.2	102.9	52.4
4	550	280.1	363.4	185.1	144.5	73.6

The variations of τ_f and τ_r with σ' are plotted in Figure 11.13. From the plots, we find that

Peak strength: $\tau_f(\text{kN/m}^2) = \mathbf{40 + \sigma' \tan 27}$

Residual strength: $\tau_r(\text{kN/m}^2) = \mathbf{\sigma' \tan 14.6}$

(*Note:* For all *overconsolidated clays,* the residual shear strength can be expressed as

$$\tau_r = \sigma' \tan \phi_r'$$

where ϕ_r' = effective residual friction angle.) ■

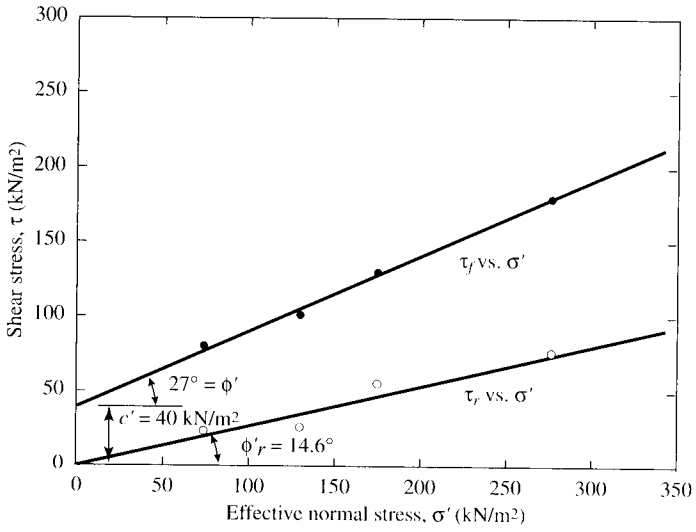

Figure 11.13 Variations of τ_f and τ_r with σ'

11.7 Triaxial Shear Test (General)

The triaxial shear test is one of the most reliable methods available for determining shear strength parameters. It is widely used for research and conventional testing. A diagram of the triaxial test layout is shown in Figure 11.14.

In this test, a soil specimen about 36 mm (1.4 in.) in diameter and 76 mm (3 in.) long is generally used. The specimen is encased by a thin rubber membrane and placed inside a plastic cylindrical chamber that is usually filled with water or glycerine. The specimen is subjected to a confining pressure by compression of the fluid in the chamber. (*Note:* Air is sometimes used as a compression medium.) To cause shear failure in the specimen, one must apply axial stress through a vertical loading ram (sometimes called *deviator stress*). This stress can be applied in one of two ways:

1. Application of dead weights or hydraulic pressure in equal increments until the specimen fails. (Axial deformation of the specimen resulting from the load applied through the ram is measured by a dial gauge.)
2. Application of axial deformation at a constant rate by means of a geared or hydraulic loading press. This is a strain-controlled test.

The axial load applied by the loading ram corresponding to a given axial deformation is measured by a proving ring or load cell attached to the ram.

Connections to measure drainage into or out of the specimen, or to measure pressure in the pore water (as per the test conditions), are also provided. The following three standard types of triaxial tests are generally conducted:

1. Consolidated-drained test or drained test (CD test)
2. Consolidated-undrained test (CU test)
3. Unconsolidated-undrained test or undrained test (UU test)

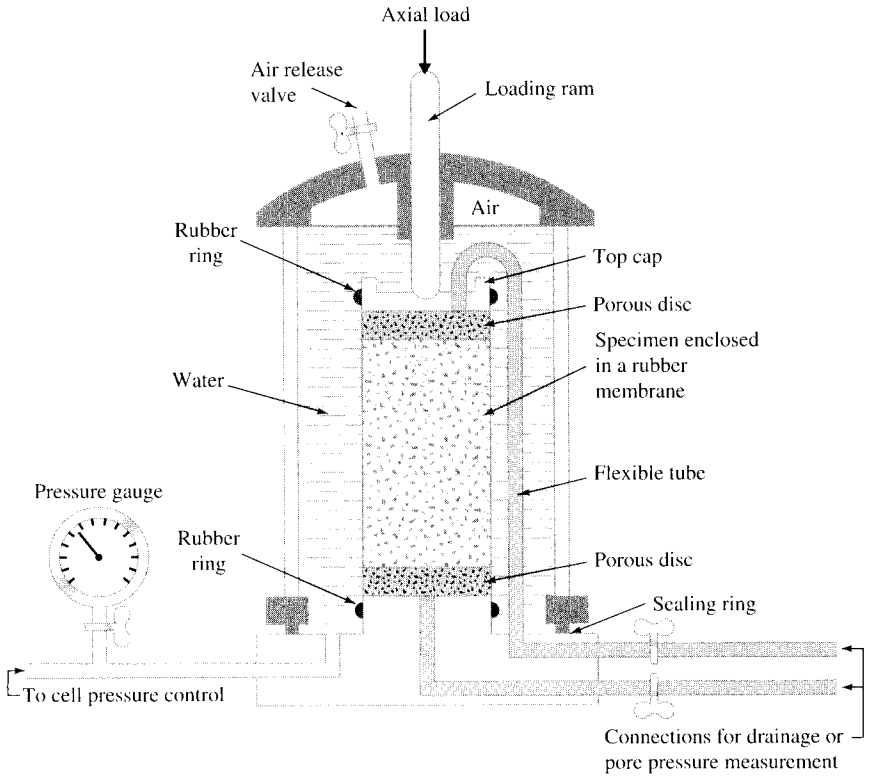

Figure 11.14 Diagram of triaxial test equipment (after Bishop and Bjerrum, 1960)

The general procedures and implications for each of the tests in *saturated soils* are described in the following sections.

11.8 Consolidated-Drained Triaxial Test

In the CD test, the saturated specimen is first subjected to an all around confining pressure, σ_3, by compression of the chamber fluid (Figure 11.15a). As confining pressure is applied, the pore water pressure of the specimen increases by u_c (if drainage is prevented). This increase in the pore water pressure can be expressed as a nondimensional parameter in the form

$$B = \frac{u_c}{\sigma_3} \tag{11.14}$$

where B = Skempton's pore pressure parameter (Skempton, 1954).

For saturated soft soils, B is approximately equal to 1; however, for saturated stiff soils, the magnitude of B can be less than 1. Black and Lee (1973) gave the theo-

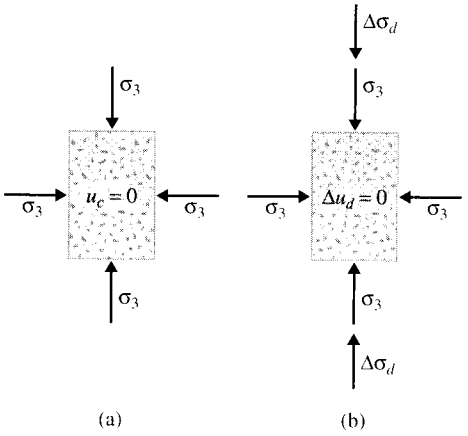

Figure 11.15
Consolidated-drained triaxial test: (a) specimen under chamber confining pressure; (b) deviator stress application

Table 11.2 Theoretical Values of B at Complete Saturation

Type of soil	Theoretical value
Normally consolidated soft clay	0.9998
Lightly overconsolidated soft clays and silts	0.9988
Overconsolidated stiff clays and sands	0.9877
Very dense sands and very stiff clays at high confining pressures	0.9130

retical values of B for various soils at complete saturation. These values are listed in Table 11.2.

Now, if the connection to drainage is opened, dissipation of the excess pore water pressure, and thus consolidation, will occur. With time, u_c will become equal to 0. In saturated soil, the change in the volume of the specimen (ΔV_c) that takes place during consolidation can be obtained from the volume of pore water drained (Figure 11.16a). Next, the deviator stress, $\Delta\sigma_d$, on the specimen is increased very slowly (Figure 11.15b). The drainage connection is kept open, and the slow rate of deviator stress application allows complete dissipation of any pore water pressure that developed as a result ($\Delta u_d = 0$).

A typical plot of the variation of deviator stress against strain in loose sand and normally consolidated clay is shown in Figure 11.16b. Figure 11.16c shows a similar plot for dense sand and overconsolidated clay. The volume change, ΔV_d, of specimens that occurs because of the application of deviator stress in various soils is also shown in Figures 11.16d and 11.16e.

Because the pore water pressure developed during the test is completely dissipated, we have

$$\text{total and effective confining stress} = \sigma_3 = \sigma_3'$$

and

$$\text{total and effective axial stress at failure} = \sigma_3 + (\Delta\sigma_d)_f = \sigma_1 = \sigma_1'$$

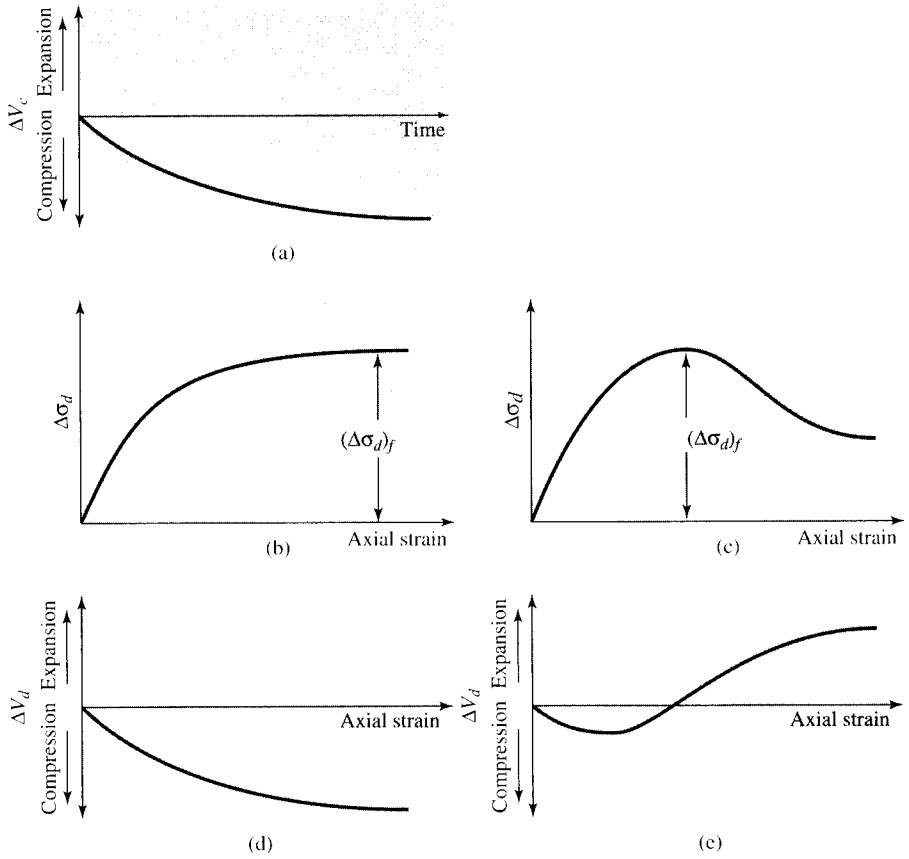

Figure 11.16 Consolidated-drained triaxial test: (a) volume change of specimen caused by chamber confining pressure; (b) plot of deviator stress against strain in the vertical direction for loose sand and normally consolidated clay; (c) plot of deviator stress against strain in the vertical direction for dense sand and overconsolidated clay; (d) volume change in loose sand and normally consolidated clay during deviator stress application; (e) volume change in dense sand and overconsolidated clay during deviator stress application

In a triaxial test, σ'_1 is the major principal effective stress at failure and σ'_3 is the minor principal effective stress at failure.

Several tests on similar specimens can be conducted by varying the confining pressure. With the major and minor principal stresses at failure for each test the Mohr's circles can be drawn and the failure envelopes can be obtained. Figure 11.17 shows the type of effective stress failure envelope obtained for tests on sand and normally consolidated clay. The coordinates of the point of tangency of the failure envelope with a Mohr's circle (that is, point A) give the stresses (normal and shear) on the failure plane of that test specimen.

Overconsolidation results when a clay is initially consolidated under an all-around chamber pressure of σ_c $(= \sigma'_c)$ and is allowed to swell by reducing the chamber pressure to σ_3 $(= \sigma'_3)$. The failure envelope obtained from drained triaxial tests of such overconsolidated clay specimens shows two distinct branches (ab and bc in

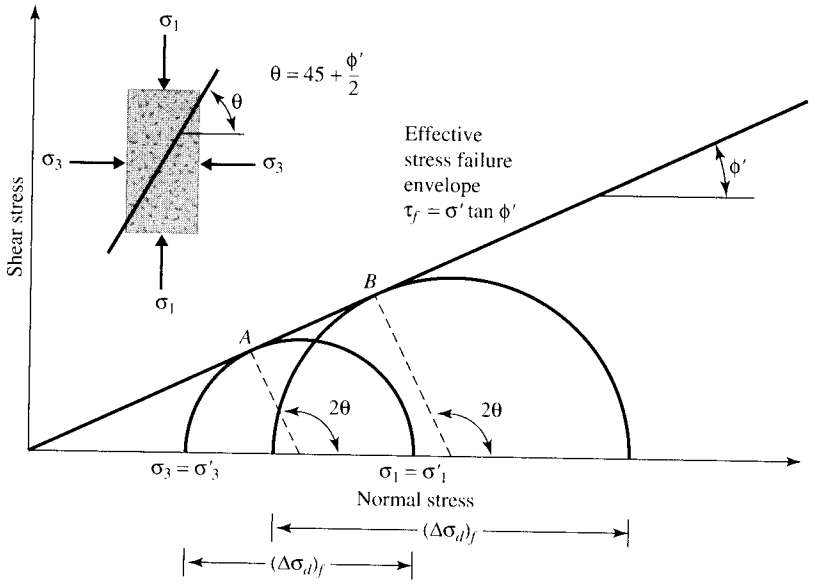

Figure 11.17 Effective stress failure envelope from drained tests on sand and normally consolidated clay

Figure 11.18). The portion *ab* has a flatter slope with a cohesion intercept, and the shear strength equation for this branch can be written as

$$\tau_f = c' + \sigma' \tan \phi'_1 \tag{11.15}$$

The portion *bc* of the failure envelope represents a normally consolidated stage of soil and follows the equation $\tau_f = \sigma' \tan \phi'$.

A consolidated-drained triaxial test on a clayey soil may take several days to complete. This amount of time is required because deviator stress must be applied very slowly to ensure full drainage from the soil specimen. For this reason, the CD type of triaxial test is uncommon.

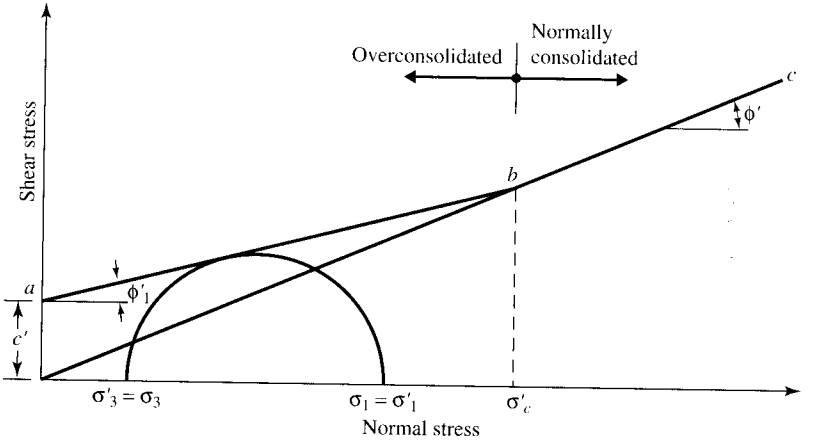

Figure 11.18 Effective stress failure envelope for overconsolidated clay

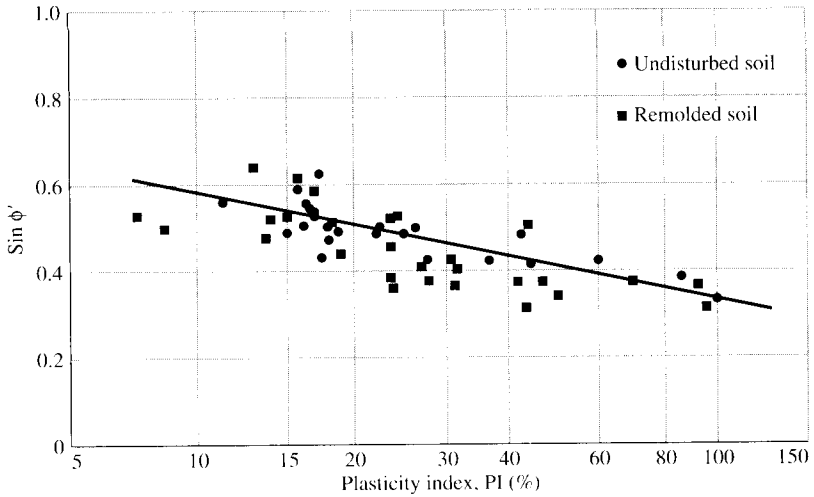

Figure 11.19 Variation of sin ϕ' with plasticity index for a number of soils (after Kenney, 1959)

Comments on Drained and Residual Friction Angles of Clay

The drained angle of friction, ϕ', generally decreases with the plasticity index of soil. This fact is illustrated in Figure 11.19 for a number of clays from data reported by Kenney (1959). Although the data are considerably scattered, the general pattern seems to hold. In Figure 11.8, the residual shear strength of clay soil is defined. Also in Example 11.1, the procedure to calculate residual friction angle ϕ'_r is shown.

Skempton (1964) provided the results of the variation of the residual angle of friction, ϕ'_r, of a number of clayey soils with the clay-size fraction ($\leq 2\ \mu$m) present. The following table shows a summary of these results:

Soil	Clay-size fraction (%)	Residual friction angle, ϕ_r (deg)
Selset	17.7	29.8
Wiener Tegel	22.8	25.1
Jackfield	35.4	19.1
Oxford clay	41.9	16.3
Jari	46.5	18.6
London clay	54.9	16.3
Walton's Wood	67	13.2
Weser-Elbe	63.2	9.3
Little Belt	77.2	11.2
Biotite	100	7.5

At a very high clay content, ϕ'_r approaches the value of the angle of sliding friction for sheet minerals. For highly plastic sodium montmorillonites, the magnitude of ϕ'_r may be as low as 3 to 4°.

Example 11.2

For a normally consolidated clay, the results of a drained triaxial test are as follows:

Chamber confining pressure = 16 lb/in.^{2}

Deviator stress at failure = 25 lb/in.^{2}

a. Find the angle of friction, ϕ'.
b. Determine the angle θ that the failure plane makes with the major principal plane.

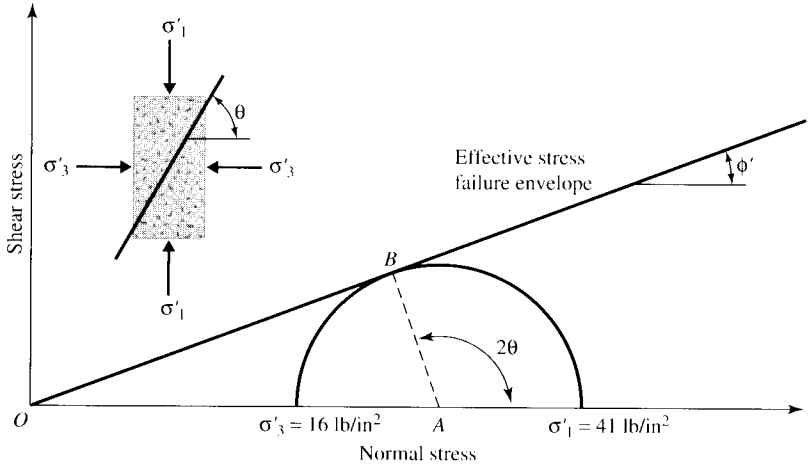

Figure 11.20 Mohr's circle and failure envelope for a normally consolidated clay

Solution

For a normally consolidated soil, the failure envelope equation is

$$\tau_f = \sigma' \tan \phi' \qquad (\text{since } c' = 0)$$

For the triaxial test, the effective major and minor principal stresses at failure are

$$\sigma_1' = \sigma_1 = \sigma_3 + (\Delta\sigma_d)_f = 16 + 25 = 41 \text{ lb/in.}^2$$

and

$$\sigma_3' = \sigma_3 = 16 \text{ lb/in.}^2$$

a. The Mohr's circle and the failure envelope are shown in Figure 11.20, from which we can write

$$\sin \phi' = \frac{AB}{OA} = \frac{\left(\dfrac{\sigma_1' - \sigma_3'}{2}\right)}{\left(\dfrac{\sigma_1' + \sigma_3'}{2}\right)}$$

or

$$\sin \phi' = \frac{\sigma_1' - \sigma_3'}{\sigma_1' + \sigma_3'} = \frac{41 - 16}{41 + 16} = 0.438$$

$$\phi' = \mathbf{26°}$$

b. $\theta = 45 + \dfrac{\phi'}{2} = 45° + \dfrac{26}{2} = \mathbf{58°}$ ■

Example 11.3

Refer to Example 11.2.

a. Find the normal stress σ' and the shear stress τ_f on the failure plane.
b. Determine the effective normal stress on the plane of maximum shear stress.

Solution

a. From Eqs. (9.8) and (9.9),

$$\sigma' \text{ (on the failure plane)} = \frac{\sigma_1' + \sigma_3'}{2} + \frac{\sigma_1' - \sigma_3'}{2} \cos 2\theta$$

and

$$\tau_f = \frac{\sigma_1' - \sigma_3'}{2} \sin 2\theta$$

Subsituting the values of $\sigma_1' = 41$ lb/in.^{2}, $\sigma_3' = 16$ lb/in.^{2}, and $\theta = 58°$ into the preceding equations, we get

$$\sigma' = \frac{41 + 16}{2} + \frac{41 - 16}{2} \cos(2 \times 58) = \mathbf{23.0\ lb/in.^2}$$

and

$$\tau_f = \frac{41 - 16}{2} \sin(2 \times 58) = \mathbf{11.2\ lb/in.^2}$$

b. From Eq. (9.9), it can be seen that the maximum shear stress will occur on the plane with $\theta = 45°$. From Eq. (9.8),

$$\sigma' = \frac{\sigma_1' + \sigma_3'}{2} + \frac{\sigma_1' - \sigma_3'}{2} \cos 2\theta$$

Substituting $\theta = 45°$ into the preceding equation gives

$$\sigma' = \frac{41 + 16}{2} + \frac{41 - 16}{2} \cos 90 = \mathbf{28.5\ lb/in.^2}$$ ■

Example 11.4

The equation of the effective stress failure envelope for normally consolidated clayey soil is $\tau_f = \sigma' \tan 25°$. A drained triaxial test was conducted with the same soil at a chamber confining pressure of 80 kN/m^2. Calculate the deviator stress at failure.

Solution

For normally consolidated clay, $c' = 0$. Thus, from Eq. (11.8),

$$\sigma_1' = \sigma_3' \tan^2\left(45 + \frac{\phi'}{2}\right)$$

$$\phi' = 25°$$

$$\sigma_1' = 80 \tan^2\left(45 + \frac{25}{2}\right) = 197 \text{ kN/m}^2$$

so

$$(\Delta\sigma_d)_f = \sigma_1' - \sigma_3' = 197 - 80 = \mathbf{117 \text{ kN/m}^2}$$ ■

Example 11.5

The results of two drained triaxial tests on a saturated clay are as follows:

Specimen I: $\sigma_3 = \sigma_3' = 70 \text{ kN/m}^2$

$(\Delta\sigma_d)_f = 130 \text{ kN/m}^2$

Specimen II: $\sigma_3 = \sigma_3' = 160 \text{ kN/m}^2$

$(\Delta\sigma_d)_f = 223.5 \text{ kN/m}^2$

Determine the shear strength parameters c' and ϕ'.

Solution

For specimen I, the principal stresses at failure are

$$\sigma_3' = \sigma_3 = 70 \text{ kN/m}^2$$

and

$$\sigma_1' = \sigma_1 = \sigma_3 + (\Delta\sigma_d)_f = 70 + 130 = 200 \text{ kN/m}^2$$

Similarly, the principal stresses at failure for specimen II are

$$\sigma_3' = \sigma_3 = 160 \text{ kN/m}^2$$

and

$$\sigma_1' = \sigma_1 = \sigma_3 + (\Delta\sigma_d)_f = 160 + 223.5 = 383.5 \text{ kN/m}^2$$

Using the relationship given by Eq. (11.8), we get

$$\sigma_1' = \sigma_3' \tan^2\left(45 + \frac{\phi'}{2}\right) + 2c' \tan\left(45 + \frac{\phi'}{2}\right)$$

Thus, for specimen I,

$$200 = 70 \tan^2\left(45 + \frac{\phi'}{2}\right) + 2c' \tan\left(45 + \frac{\phi'}{2}\right)$$

and for specimen II,

$$383.5 = 160 \tan^2\left(45 + \frac{\phi'}{2}\right) + 2c' \tan\left(45 + \frac{\phi'}{2}\right)$$

Solving the two preceding equations, we obtain

$$\phi' = 20^\circ \qquad c' = \mathbf{20\ kN/m^2}$$

■

11.9 Consolidated-Undrained Triaxial Test

The consolidated-undrained test is the most common type of triaxial test. In this test, the saturated soil specimen is first consolidated by an all-around chamber fluid pressure, σ_3, that results in drainage (Figures 11.21a and 11.21b). After the pore water pressure generated by the application of confining pressure is dissipated, the deviator stress, $\Delta\sigma_d$, on the specimen is increased to cause shear failure (Figure 11.21c). During this phase of the test, the drainage line from the specimen is kept closed. Because drainage is not permitted, the pore water pressure, Δu_d, will increase. During the test, simultaneous measurements of $\Delta\sigma_d$ and Δu_d are made. The increase in the pore water pressure, Δu_d, can be expressed in a nondimensional form as

$$\overline{A} = \frac{\Delta u_d}{\Delta \sigma_d} \tag{11.16}$$

where $\overline{A}$ = Skempton's pore pressure parameter (Skempton, 1954).

The general patterns of variation of $\Delta\sigma_d$ and Δu_d with axial strain for sand and clay soils are shown in Figures 11.21d through 11.21g. In loose sand and normally consolidated clay, the pore water pressure increases with strain. In dense sand and overconsolidated clay, the pore water pressure increases with strain to a certain limit, beyond which it decreases and becomes negative (with respect to the atmospheric pressure). This decrease is because of a tendency of the soil to dilate.

Unlike the consolidated-drained test, the total and effective principal stresses are not the same in the consolidated-undrained test. Because the pore water pressure at failure is measured in this test, the principal stresses may be analyzed as follows:

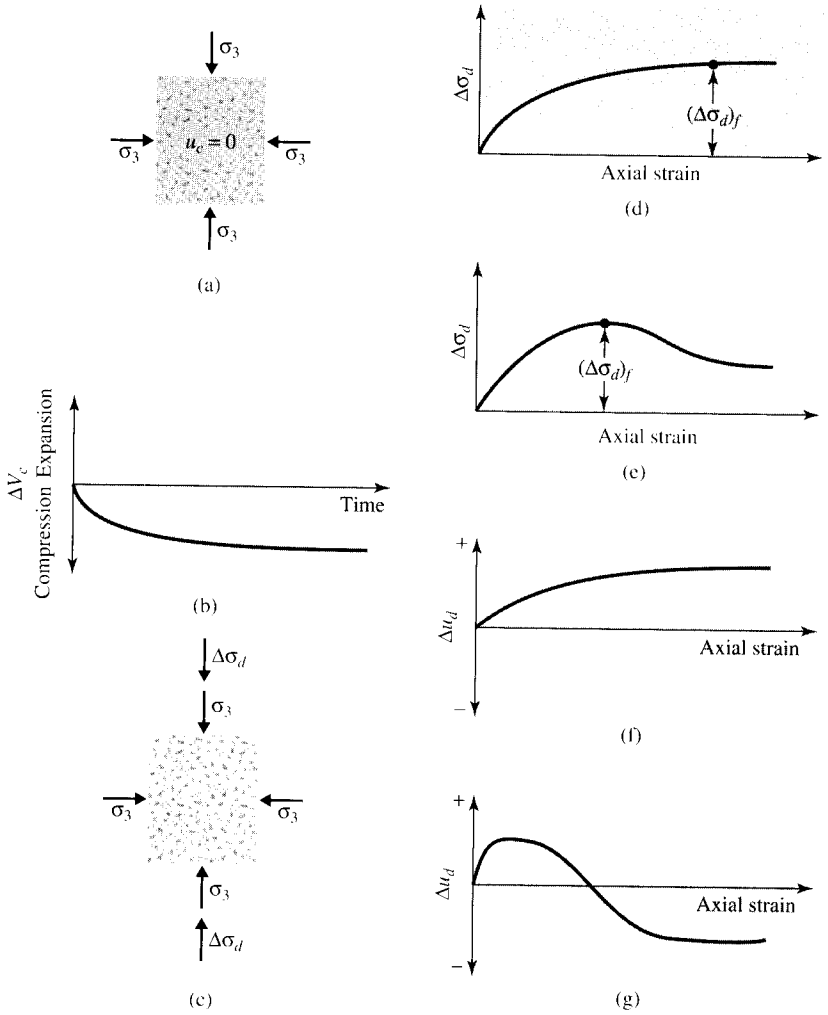

Figure 11.21 Consolidated undrained test: (a) specimen under chamber confining pressure; (b) volume change in specimen caused by confining pressure; (c) deviator stress application; (d) deviator stress against axial strain for loose sand and normally consolidated clay; (e) deviator stress against axial strain for dense sand and overconsolidated clay; (f) variation of pore water pressure with axial strain for loose sand and normally consolidated clay; (g) variation of pore water pressure with axial strain for dense sand and overconsolidated clay

- Major principal stress at failure (total): $\sigma_3 + (\Delta\sigma_d)_f = \sigma_1$
- Major principal stress at failure (effective): $\sigma_1 - (\Delta u_d)_f = \sigma'_1$
- Minor principal stress at failure (total): σ_3
- Minor principal stress at failure (effective): $\sigma_3 - (\Delta u_d)_f = \sigma'_3$

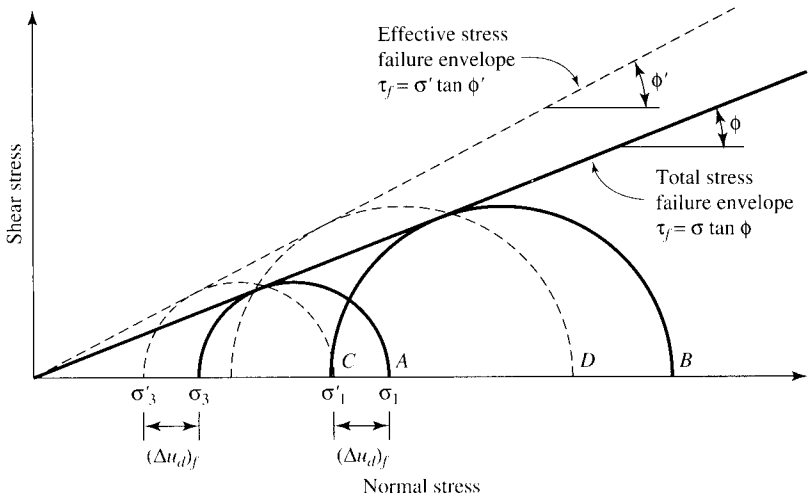

Figure 11.22 Total and effective stress failure envelopes for consolidated undrained triaxial tests. (*Note:* The figure assumes that no back pressure is applied.)

In these equations, $(\Delta u_d)_f$ = pore water pressure at failure. The preceding derivations show that

$$\sigma_1 - \sigma_3 = \sigma'_1 - \sigma'_3$$

Tests on several similar specimens with varying confining pressures may be conducted to determine the shear strength parameters. Figure 11.22 shows the total and effective stress Mohr's circles at failure obtained from consolidated-undrained triaxial tests in sand and normally consolidated clay. Note that A and B are two total stress Mohr's circles obtained from two tests. C and D are the effective stress Mohr's circles corresponding to total stress circles A and B, respectively. The diameters of circles A and C are the same; similarly, the diameters of circles B and D are the same.

In Figure 11.22, the total stress failure envelope can be obtained by drawing a line that touches all the total stress Mohr's circles. For sand and normally consolidated clays, this will be approximately a straight line passing through the origin and may be expressed by the equation

$$\tau_f = \sigma \tan \phi \tag{11.17}$$

where σ = total stress
ϕ = the angle that the total stress failure envelope makes with the normal stress axis, also known as the *consolidated-undrained angle of shearing resistance*

Equation (11.17) is seldom used for practical considerations.

Again referring to Figure 11.22, we see that the failure envelope that is tangent to all the effective stress Mohr's circles can be represented by the equation $\tau_f = \sigma' \tan \phi'$, which is the same as that obtained from consolidated-drained tests (see Figure 11.17).

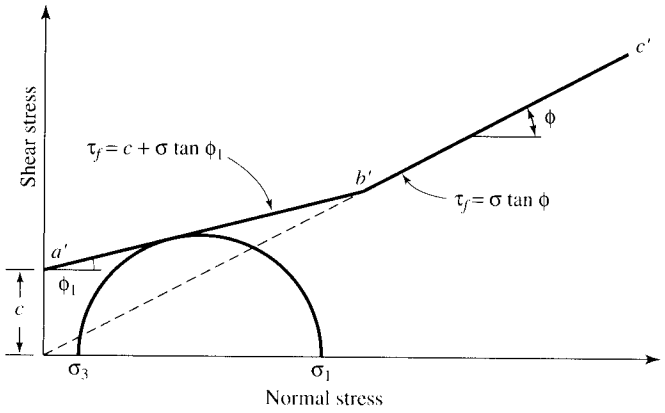

Figure 11.23 Total stress failure envelope obtained from consolidated-undrained tests in over-consolidated clay

In overconsolidated clays, the total stress failure envelope obtained from consolidated-undrained tests will take the shape shown in Figure 11.23. The straight line $a'b'$ is represented by the equation

$$\tau_f = c + \sigma \tan \phi_1 \tag{11.18}$$

and the straight line $b'c'$ follows the relationship given by Eq. (11.17). The effective stress failure envelope drawn from the effective stress Mohr's circles will be similar to that shown in Figure 11.23.

Consolidated-drained tests on clay soils take considerable time. For this reason, consolidated-undrained tests can be conducted on such soils with pore pressure measurements to obtain the drained shear strength parameters. Because drainage is not allowed in these tests during the application of deviator stress, they can be performed quickly.

Skempton's pore water pressure parameter $\overline{A}$ was defined in Eq. (11.16). At failure, the parameter $\overline{A}$ can be written as

$$\overline{A} = \overline{A}_f = \frac{(\Delta u_d)_f}{(\Delta \sigma_d)_f} \tag{11.19}$$

The general range of $\overline{A}_f$ values in most clay soils is as follows:

- Normally consolidated clays: 0.5 to 1
- Overconsolidated clays: −0.5 to 0

Table 11.3 gives the values of $\overline{A}_f$ for some normally consolidated clays as obtained by the Norwegian Geotechnical Institute.

Laboratory triaxial tests of Bjerrum and Simons (1960) on Oslo clay, Weald clay, and London clay showed that $\overline{A}_f$ becomes approximately zero at an overconsolidation value of about 3 or 4.

Table 11.3 Triaxial Test Results for Some Normally Consolidated Clays Obtained by the Norwegian Geotechnical Institute*

Location	Liquid limit	Plastic limit	Liquidity index	Sensitivity[a]	Drained friction angle, ϕ' (deg)	$\bar{A}_f$
Seven Sisters, Canada	127	35	0.28		19	0.72
Sarpborg	69	28	0.68	5	25.5	1.03
Lilla Edet, Sweden	68	30	1.32	50	26	1.10
Fredrikstad	59	22	0.58	5	28.5	0.87
Fredrikstad	57	22	0.63	6	27	1.00
Lilla Edet, Sweden	63	30	1.58	50	23	1.02
Göta River, Sweden	60	27	1.30	12	28.5	1.05
Göta River, Sweden	60	30	1.50	40	24	1.05
Oslo	48	25	0.87	4	31.5	1.00
Trondheim	36	20	0.50	2	34	0.75
Drammen	33	18	1.08	8	28	1.18

* After Bjerrum and Simons (1960)
[a] See Section 11.15 for the definition of sensitivity.

Example 11.6

A consolidated-undrained test on a normally consolidated clay yielded the following results:

$\sigma_3 = 12$ lb/in.^{2}

Deviator stress, $(\Delta\sigma_d)_f = 9.1$ lb/in.^{2}

Pore pressure, $(\Delta u_d)_f = 6.8$ lb/in.^{2}

Calculate the consolidated-undrained friction angle and the consolidated-drained friction angle.

Solution

$$\sigma_3 = 12 \text{ lb/in.}^2$$

$$\sigma_1 = \sigma_3 + (\Delta\sigma_d)_f = 12 + 9.1 = 21.1 \text{ lb/in.}^2$$

From Eq. (11.9), for normally consolidated clay with $c = 0$,

$$\sigma_1 = \sigma_3 \tan^2\left(45 + \frac{\phi}{2}\right)$$

$$21.1 = 12 \tan^2\left(45 + \frac{\phi}{2}\right)$$

$$\phi = 2\left[\tan^{-1}\left(\frac{21.1}{12}\right)^{0.5} - 45\right] = \mathbf{16°}$$

Again,

$$\sigma_3' = \sigma_3 - (\Delta u_d)_f = 12 - 6.8 = 5.2 \text{ lb/in.}^2$$

$$\sigma_1' = \sigma_1 - (\Delta u_d)_f = 21.1 - 6.8 = 14.3 \text{ lb/in.}^2$$

From Eq. (11.8), for normally consolidated clay with $c' = 0$,

$$\sigma_1' = \sigma_3' \tan^2\left(45 + \frac{\phi'}{2}\right)$$

$$14.3 = 5.2 \tan^2\left(45 + \frac{\phi'}{2}\right)$$

$$\phi' = 2\left[\tan^{-1}\left(\frac{14.3}{5.2}\right)^{0.5} - 45\right] = \mathbf{27.8°}$$

■

11.10 Unconsolidated-Undrained Triaxial Test

In unconsolidated-undrained tests, drainage from the soil specimen is not permitted during the application of chamber pressure σ_3. The test specimen is sheared to failure by the application of deviator stress, $\Delta\sigma_d$, and drainage is prevented. Because drainage is not allowed at any stage, the test can be performed quickly. Because of the application of chamber confining pressure σ_3, the pore water pressure in the soil specimen will increase by u_c. A further increase in the pore water pressure (Δu_d) will occur because of the deviator stress application. Hence, the total pore water pressure u in the specimen at any stage of deviator stress application can be given as

$$u = u_c + \Delta u_d \tag{11.20}$$

From Eqs. (11.14) and (11.16), $u_c = B\sigma_3$ and $\Delta u_d = \overline{A}\Delta\sigma_d$, so

$$u = B\sigma_3 + \overline{A}\Delta\sigma_d = B\sigma_3 + \overline{A}(\sigma_1 - \sigma_3) \tag{11.21}$$

This test is usually conducted on clay specimens and depends on a very important strength concept for cohesive soils if the soil is fully saturated. The added axial stress at failure $(\Delta\sigma_d)_f$ is practically the same regardless of the chamber confining pressure. This property is shown in Figure 11.24. The failure envelope for the total stress Mohr's circles becomes a horizontal line and hence is called a $\phi = 0$ condition. From Eq. (11.9) with $\phi = 0$, we get

$$\tau_f = c = c_u \tag{11.22}$$

where c_u is the undrained shear strength and is equal to the radius of the Mohr's circles. Note that the $\phi = 0$ concept is applicable to only saturated clays and silts.

The reason for obtaining the same added axial stress $(\Delta\sigma_d)_f$ regardless of the confining pressure can be explained as follows. If a clay specimen (no. 1) is consoli-

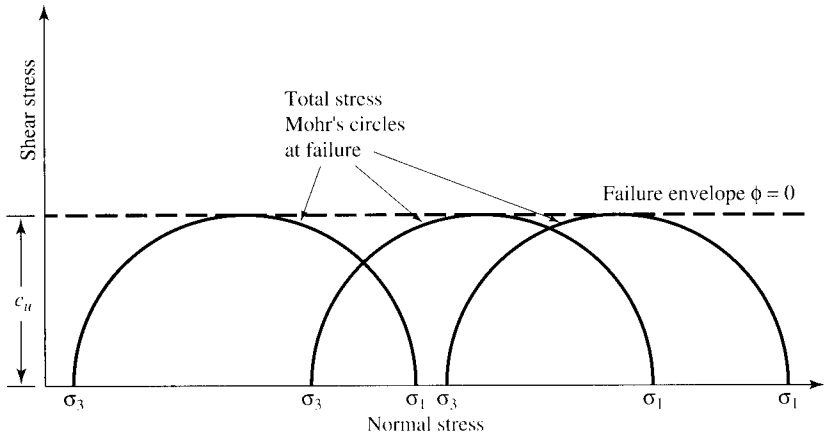

Figure 11.24 Total stress Mohr's circles and failure envelope ($\phi = 0$) obtained from unconsolidated-undrained triaxial tests on fully saturated cohesive soil

dated at a chamber pressure σ_3 and then sheared to failure without drainage, the total stress conditions at failure can be represented by the Mohr's circle P in Figure 11.25. The pore pressure developed in the specimen at failure is equal to $(\Delta u_d)_f$. Thus, the major and minor principal effective stresses at failure are, respectively,

$$\sigma_1' = [\sigma_3 + (\Delta\sigma_d)_f] - (\Delta u_d)_f = \sigma_1 - (\Delta u_d)_f$$

and

$$\sigma_3' = \sigma_3 - (\Delta u_d)_f$$

Q is the effective stress Mohr's circle drawn with the preceding principal stresses. Note that the diameters of circles P and Q are the same.

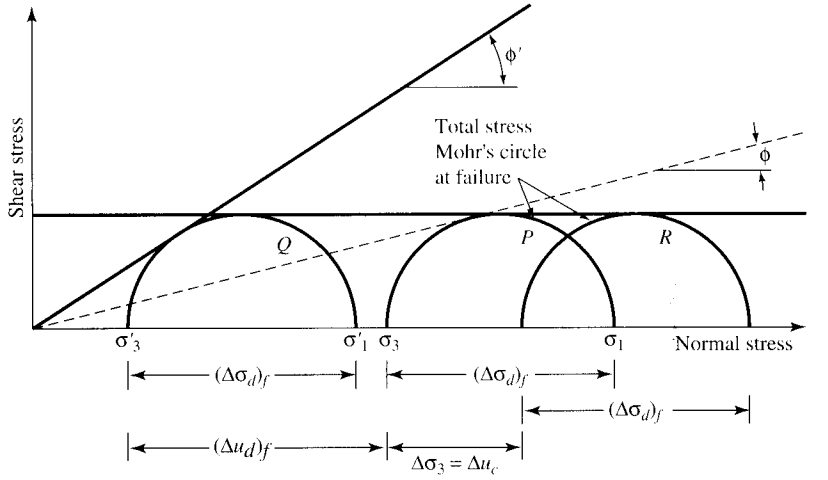

Figure 11.25 The $\phi = 0$ concept

Now let us consider another similar clay specimen (no. II) that has been consolidated under a chamber pressure σ_3 with initial pore pressure equal to zero. If the chamber pressure is increased by $\Delta\sigma_3$ without drainage, the pore water pressure will increase by an amount Δu_c. For saturated soils under isotropic stresses, the pore water pressure increase is equal to the total stress increase, so $\Delta u_c = \Delta\sigma_3$ ($B = 1$). At this time, the effective confining pressure is equal to $\sigma_3 + \Delta\sigma_3 - \Delta u_c = \sigma_3 + \Delta\sigma_3 - \Delta\sigma_3 = \sigma_3$. This is the same as the effective confining pressure of specimen no. I before the application of deviator stress. Hence, if specimen no. II is sheared to failure by increasing the axial stress, it should fail at the same deviator stress $(\Delta\sigma_d)_f$ that was obtained for specimen no. I. The total stress Mohr's circle at failure will be R (see Figure 11.25). The added pore pressure increase caused by the application of $(\Delta\sigma_d)_f$ will be $(\Delta u_d)_f$.

At failure, the minor principal effective stress is

$$[(\sigma_3 + \Delta\sigma_3)] - [\Delta u_c + (\Delta u_d)_f] = \sigma_3 - (\Delta u_d)_f = \sigma'_3$$

and the major principal effective stress is

$$[\sigma_3 + \Delta\sigma_3 + (\Delta\sigma_d)_f] - [\Delta u_c + (\Delta u_d)_f] = [\sigma_3 + (\Delta\sigma_d)_f] - (\Delta u_d)_f$$
$$= \sigma_1 - (\Delta u_d)_f = \sigma'_1$$

Thus, the effective stress Mohr's circle will still be Q because strength is a function of effective stress. Note that the diameters of circles P, Q, and R are all the same.

Any value of $\Delta\sigma_3$ could have been chosen for testing specimen no. II. In any case, the deviator stress $(\Delta\sigma_d)_f$ to cause failure would have been the same as long as the soil was fully saturated and fully undrained during both stages of the test.

11.11 Unconfined Compression Test on Saturated Clay

The unconfined compression test is a special type of unconsolidated-undrained test that is commonly used for clay specimens. In this test, the confining pressure σ_3 is 0. An axial load is rapidly applied to the specimen to cause failure. At failure, the total minor principal stress is zero and the total major principal stress is σ_1 (Figure 11.26).

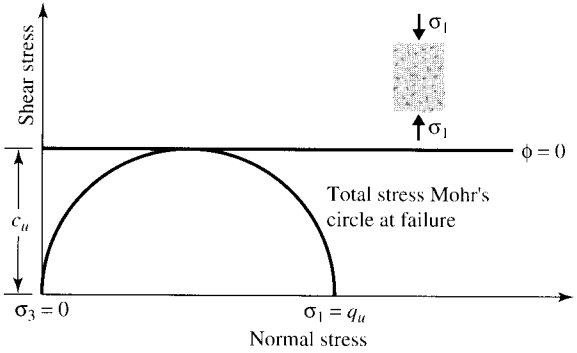

Figure 11.26 Unconfined compression test

Table 11.4 General Relationship of Consistency and Unconfined Compression Strength of Clays

Consistency	q_u kN/m²	q_u ton/ft²
Very soft	0–25	0–0.25
Soft	25–50	0.25–0.5
Medium	50–100	0.5–1
Stiff	100–200	1–2
Very stiff	200–400	2–4
Hard	>400	>4

Because the undrained shear strength is independent of the confining pressure as long as the soil is fully saturated and fully undrained, we have

$$\tau_f = \frac{\sigma_1}{2} = \frac{q_u}{2} = c_u \tag{11.23}$$

where q_u is the *unconfined compression strength.* Table 11.4 gives the approximate consistencies of clays on the basis of their unconfined compression strength. A photograph of unconfined compression test equipment is shown in Figure 11.27.

Theoretically, for similar saturated clay specimens, the unconfined compression tests and the unconsolidated-undrained triaxial tests should yield the same values of c_u. In practice, however, unconfined compression tests on saturated clays yield slightly lower values of c_u than those obtained from unconsolidated-undrained tests.

11.12 Stress Path

Results of triaxial tests can be represented by diagrams called *stress paths.* A stress path is a line that connects a series of points, each of which represents a successive stress state experienced by a soil specimen during the progress of a test. There are several ways in which a stress path can be drawn. This section covers one of them.

Lambe (1964) suggested a type of stress path representation that plots q' against p' (where p' and q' are the coordinates of the top of the Mohr's circle). Thus, relationships for p' and q' are as follows:

$$p' = \frac{\sigma_1' + \sigma_3'}{2} \tag{11.24}$$

$$q' = \frac{\sigma_1' - \sigma_3'}{2} \tag{11.25}$$

This type of stress path plot can be explained with the aid of Figure 11.28. Let us consider a normally consolidated clay specimen subjected to an isotropically

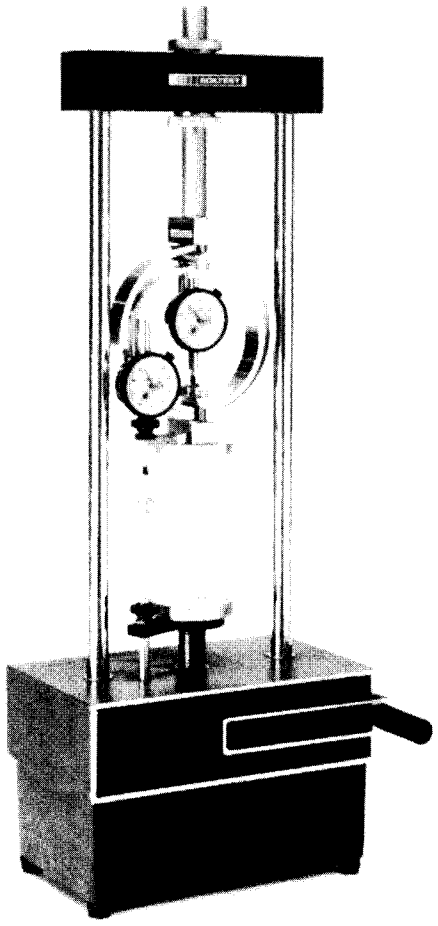

Figure 11.27
Unconfined compression test equipment (courtesy of Soiltest, Inc., Lake Bluff, Illinois)

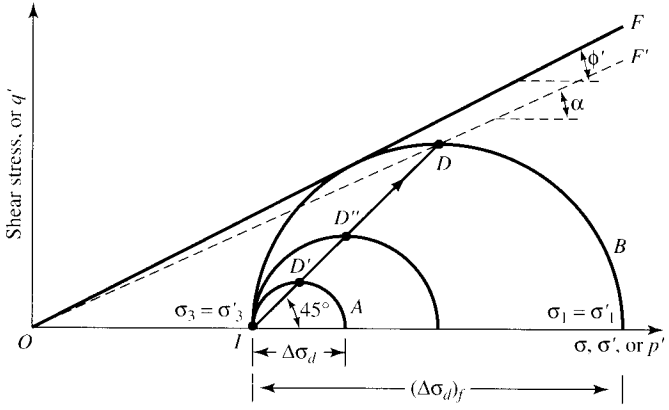

Figure 11.28 Stress path — plot of q' against p' for a consolidated-drained triaxial test on a normally consolidated clay

consolidated-drained triaxial test. At the beginning of the application of deviator stress, $\sigma'_1 = \sigma'_3 = \sigma_3$, so

$$p' = \frac{\sigma'_3 + \sigma'_3}{2} = \sigma'_3 = \sigma_3 \tag{11.26}$$

and

$$q' = \frac{\sigma'_3 - \sigma'_3}{2} = 0 \tag{11.27}$$

For this condition, p' and q' will plot as a point (that is, I in Figure 11.28). At some other time during deviator stress application, $\sigma'_1 = \sigma'_3 + \Delta\sigma_d = \sigma_3 + \Delta\sigma_d$; $\sigma'_3 = \sigma_3$. The Mohr's circle marked A in Figure 11.28 corresponds to this state of stress on the soil specimen. The values of p' and q' for this stress condition are

$$p' = \frac{\sigma'_1 + \sigma'_3}{2} = \frac{(\sigma'_3 + \Delta\sigma_d) + \sigma'_3}{2} = \sigma'_3 + \frac{\Delta\sigma_d}{2} = \sigma_3 + \frac{\Delta\sigma_d}{2} \tag{11.28}$$

and

$$q' = \frac{(\sigma'_3 + \Delta\sigma_d) - \sigma'_3}{2} = \frac{\Delta\sigma_d}{2} \tag{11.29}$$

If these values of p' and q' were plotted in Figure 11.28, they would be represented by point D' at the top of the Mohr's circle. So, if the values of p' and q' at various stages of the deviator stress application are plotted and these points are joined, a straight line like ID will result. The straight line ID is referred to as the *stress path* in a q'-p' plot for a consolidated-drained triaxial test. Note that the line ID makes an angle of 45° with the horizontal. Point D represents the failure condition of the soil specimen in the test. Also, we can see that Mohr's circle B represents the failure stress condition.

For normally consolidated clays, the failure envelope can be given by $\tau_f = \sigma' \tan \phi'$. This is the line OF in Figure 11.28. (See also Figure 11.17.) A modified failure envelope can now be defined by line OF'. This modified line is commonly called the K_f line. The equation of the K_f line can be expressed as

$$q' = p' \tan \alpha \tag{11.30}$$

where α = the angle that the modified failure envelope makes with the horizontal.

The relationship between the angles ϕ' and α can be determined by referring to Figure 11.29, in which, for clarity, the Mohr's circle at failure (that is, circle B) and lines OF and OF' as shown in Figure 11.28 have been redrawn. Note that O' is the center of the Mohr's circle at failure. Now,

$$\frac{DO'}{OO'} = \tan \alpha$$

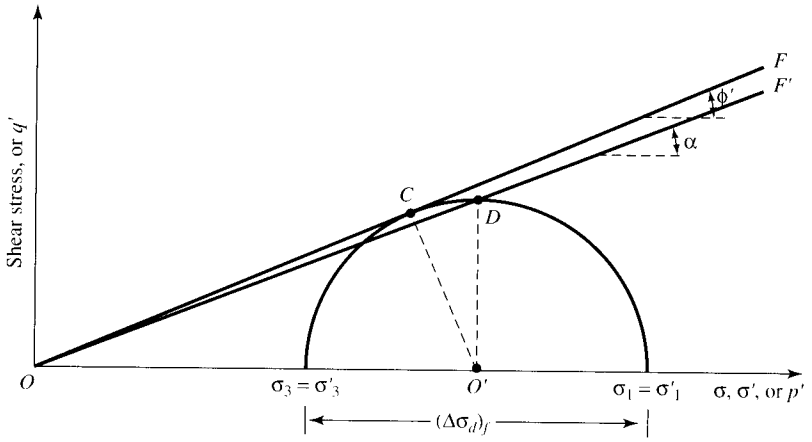

Figure 11.29 Relationship between ϕ' and α

and thus, we obtain

$$\tan \alpha = \frac{\dfrac{\sigma'_1 - \sigma'_3}{2}}{\dfrac{\sigma'_1 + \sigma'_3}{2}} = \frac{\sigma'_1 - \sigma'_3}{\sigma'_1 + \sigma'_3} \tag{11.31}$$

Again,

$$\frac{CO'}{OO'} = \sin \phi'$$

or

$$\sin \phi' = \frac{\dfrac{\sigma'_1 - \sigma'_3}{2}}{\dfrac{\sigma'_1 + \sigma'_3}{2}} = \frac{\sigma'_1 - \sigma'_3}{\sigma'_1 + \sigma'_3} \tag{11.32}$$

Comparing Eqs. (11.31) and (11.32), we see that

$$\sin \phi' = \tan \alpha \tag{11.33}$$

or

$$\phi' = \sin^{-1}(\tan \alpha) \tag{11.34}$$

Figure 11.30 shows a q'-p' plot for a normally consolidated clay specimen subjected to an isotropically consolidated-undrained triaxial test. At the beginning of the

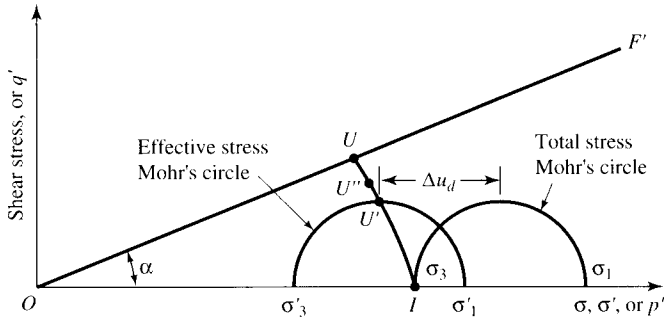

Figure 11.30 Stress path — plot of q' against p' for a consolidated-undrained triaxial test on a normally consolidated clay

application of deviator stress, $\sigma'_1 = \sigma'_3 = \sigma_3$. Hence, $p' = \sigma'_3$ and $q' = 0$. This relationship is represented by point I. At some other stage of the deviator stress application,

$$\sigma'_1 = \sigma_3 + \Delta\sigma_d - \Delta u_d$$

and

$$\sigma'_3 = \sigma_3 - \Delta u_d$$

So

$$p' = \frac{\sigma'_1 + \sigma'_3}{2} = \sigma_3 + \frac{\Delta\sigma_d}{2} - \Delta u_d \tag{11.35}$$

and

$$q' = \frac{\sigma'_1 - \sigma'_3}{2} = \frac{\Delta\sigma_d}{2} \tag{11.36}$$

The preceding values of p' and q' will plot as point U' in Figure 11.30. Points such as U'' represent values of p' and q' as the test progresses. At failure of the soil specimen,

$$p' = \sigma_3 + \frac{(\Delta\sigma_d)_f}{2} - (\Delta u_d)_f \tag{11.37}$$

and

$$q' = \frac{(\Delta\sigma_d)_f}{2} \tag{11.38}$$

The values of p' and q' given by Eqs. (11.37) and (11.38) will plot as point U. Hence, the effective stress path for a consolidated-undrained test can be given by the curve $IU'U$. Note that point U will fall on the modified failure envelope, OF' (see Figure 11.29), which is inclined at an angle α to the horizontal. Lambe (1964) proposed a technique to evaluate the elastic and consolidation settlements of foundations on clay soils by using the stress paths determined in this manner.

Example 11.7

For a normally consolidated clay, the failure envelope is given by the equation $\tau_f = \sigma' \tan \phi'$. The corresponding modified failure envelope (q'-p' plot) is given by Eq. (11.30) as $q' = p' \tan \alpha$. In a similar manner, if the failure envelope is $\tau_f = c' + \sigma' \tan \phi'$, the corresponding modified failure envelope is a q'-p' plot that can be expressed as $q' = m + p' \tan \alpha$. Express α as a function of ϕ', and give m as a function of c' and ϕ'.

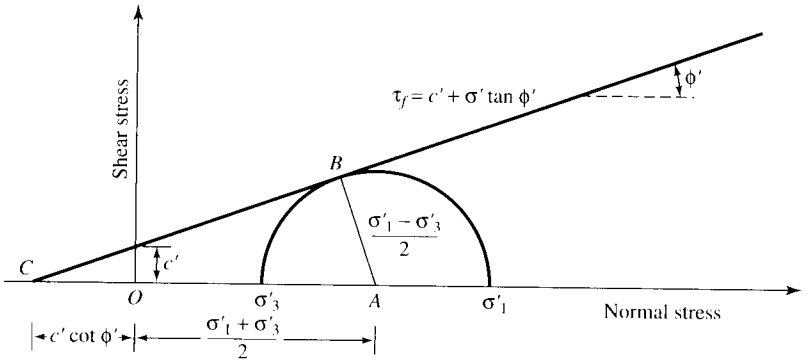

Figure 11.31 Derivation of α as a function of ϕ' and m as a function of c' and ϕ'

Solution

From Figure 11.31,

$$\sin \phi' = \frac{AB}{AC} = \frac{AB}{CO + OA} = \frac{\left(\dfrac{\sigma'_1 - \sigma'_3}{2}\right)}{c' \cot \phi' + \left(\dfrac{\sigma'_1 + \sigma'_3}{2}\right)}$$

so

$$\frac{\sigma'_1 - \sigma'_3}{2} = c' \cos \phi' + \left(\frac{\sigma'_1 + \sigma'_3}{2}\right) \sin \phi' \qquad \text{(a)}$$

or

$$q' = m + p' \tan \alpha \qquad \text{(b)}$$

Comparing Eqs. (a) and (b), we find that

$$m = \boldsymbol{c' \cos \phi'}$$

and

$$\tan \alpha = \sin \phi'$$

or

$$\alpha = \boldsymbol{\tan^{-1}(\sin \phi')}$$

■

11.13 Vane Shear Test

Fairly reliable results for the undrained shear strength, c_u ($\phi = 0$ concept), of very soft to medium cohesive soils may be obtained directly from vane shear tests. The shear vane usually consists of four thin, equal-sized steel plates welded to a steel torque rod (Figure 11.32). First, the vane is pushed into the soil. Then torque is applied at the top of the torque rod to rotate the vane at a uniform speed. A cylinder of soil of height h and diameter d will resist the torque until the soil fails. The undrained shear strength of the soil can be calculated as follows.

If T is the maximum torque applied at the head of the torque rod to cause failure, it should be equal to the sum of the resisting moment of the shear force along the side surface of the soil cylinder (M_s) and the resisting moment of the shear force at each end (M_e) (Figure 11.33):

$$T = M_s + \underbrace{M_e + M_e}_{\text{Two ends}} \tag{11.39}$$

The resisting moment can be given as

$$M_s = \underbrace{(\pi dh)c_u}_{\substack{\text{Surface} \\ \text{area}}} \underbrace{(d/2)}_{\substack{\text{Moment} \\ \text{arm}}} \tag{11.40}$$

where d = diameter of the shear vane
h = height of the shear vane

For the calculation of M_e, investigators have assumed several types of distribution of shear strength mobilization at the ends of the soil cylinder:

1. *Triangular.* Shear strength mobilization is c_u at the periphery of the soil cylinder and decreases linearly to zero at the center.
2. *Uniform.* Shear strength mobilization is constant (that is, c_u) from the periphery to the center of the soil cylinder.
3. *Parabolic.* Shear strength mobilization is c_u at the periphery of the soil cylinder and decreases parabolically to zero at the center.

These variations in shear strength mobilization are shown in Figure 11.33b. In general, the torque, T, at failure can be expressed as

$$T = \pi c_u \left[\frac{d^2h}{2} + \beta\frac{d^3}{4}\right] \tag{11.41}$$

or

$$c_u = \frac{T}{\pi\left[\dfrac{d^2h}{2} + \beta\dfrac{d^3}{4}\right]} \tag{11.42}$$

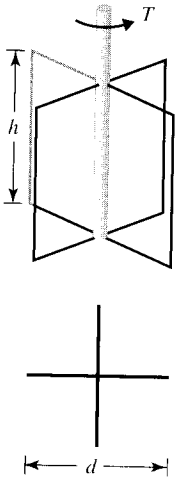

Figure 11.32
Diagram of vane shear test equipment

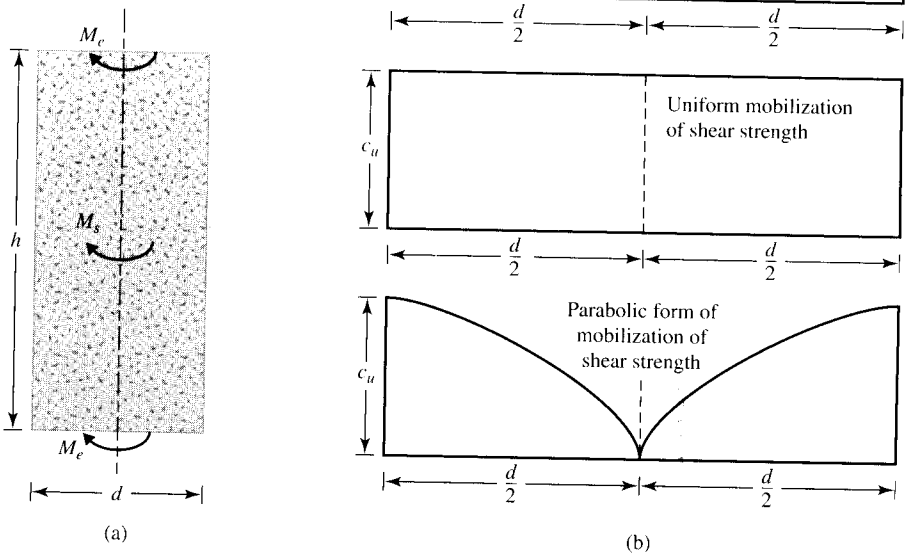

Figure 11.33 Derivation of Eq. (11.42): (a) resisting moment of shear force; (b) variations in shear strength mobilization

where $\beta = \frac{1}{2}$ for triangular mobilization of undrained shear strength
$\beta = \frac{2}{3}$ for uniform mobilization of undrained shear strength
$\beta = \frac{3}{5}$ for parabolic mobilization of undrained shear strength

Note that Eq. (11.42) is usually referred to as *Calding's equation.*

Vane shear tests can be conducted in the laboratory and in the field during soil exploration. The laboratory shear vane has dimensions of about 13 mm ($\frac{1}{2}$ in.) in diameter and 25 mm (1 in.) in height. Figure 11.34 shows a photograph of laboratory vane shear test equipment. Figure 11.35 shows the field vanes recommended by ASTM (1994). Table 11.5 gives the ASTM recommended dimensions of field vanes.

According to ASTM (1994), if $h/d = 2$, then

$$c_u(\text{kN/m}^2) = \frac{T\ (\text{N} \cdot \text{m})}{(366 \times 10^{-8})d^3} \qquad (11.43)$$

(cm)

and

$$c_u(\text{lb/ft}^2) = \frac{T\ (\text{lb} \cdot \text{ft})}{0.0021d^3} \qquad (11.44)$$

(in.)

In the field, where considerable variation in the undrained shear strength can be found with depth, vane shear tests are extremely useful. In a short period, one can establish a reasonable pattern of the change of c_u with depth. However, if the clay deposit at a given site is more or less uniform, a few unconsolidated-undrained triaxial

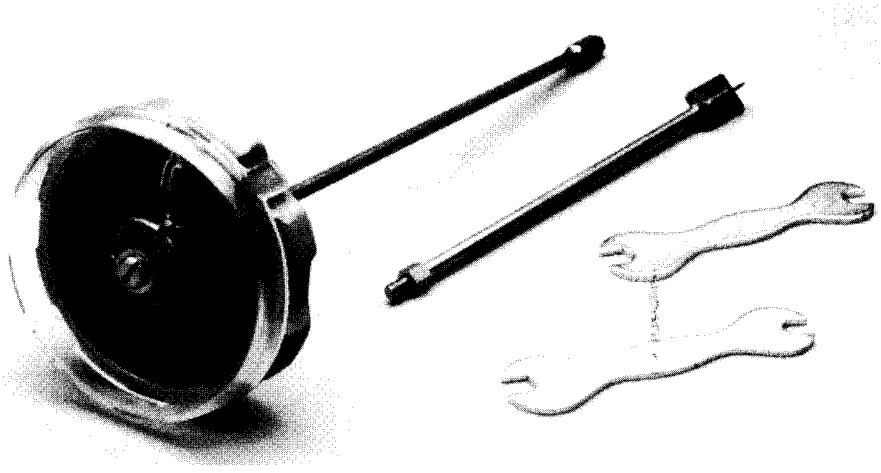

Figure 11.34 Laboratory vane shear test device (courtesy of Soiltest, Inc., Lake Bluff, Illinois)

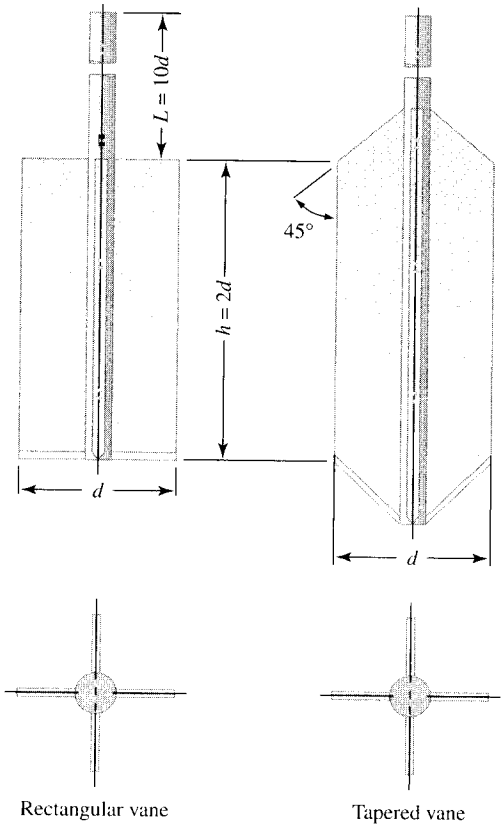

Figure 11.35 Geometry of field vanes [*Source:* From *Annual Book of ASTM Standards,* 04.08, p. 346. Copyright © 1994 American Society for Testing and Materials. Reprinted with permission]

Table 11.5 Recommended Dimensions of Field Vanes*[a]

Casing size	Diameter, mm (in.)	Height, mm (in.)	Thickness of blade, mm (in.)	Diameter of rod mm (in.)
AX	38.1 ($1\frac{1}{2}$)	76.2 (3)	1.6 ($\frac{1}{16}$)	12.7 ($\frac{1}{2}$)
BX	50.8 (2)	101.6 (4)	1.6 ($\frac{1}{16}$)	12.7 ($\frac{1}{2}$)
NX	63.5 ($2\frac{1}{2}$)	127.0 (5)	3.2 ($\frac{1}{8}$)	12.7 ($\frac{1}{2}$)
101.6 mm (4 in.)[b]	92.1 ($3\frac{5}{8}$)	184.1 ($7\frac{1}{4}$)	3.2 ($\frac{1}{8}$)	12.7 ($\frac{1}{2}$)

*After ASTM, 1994

[a]Selection of vane size is directly related to the consistency of the soil being tested; that is, the softer the soil, the larger the vane diameter should be.

[b]Inside diameter

tests on undisturbed specimens will allow a reasonable estimation of soil parameters for design work. Vane shear tests are also limited by the strength of soils in which they can be used. The undrained shear strength obtained from a vane shear test also depends on the rate of application of torque T.

Bjerrum (1974) showed that as the plasticity of soils increases, c_u obtained from vane shear tests may give results that are unsafe for foundation design. For this reason, he suggested the correction

$$c_{u(\text{design})} = \lambda c_{u(\text{vane shear})} \tag{11.45}$$

where

$$\lambda = \text{correction factor} = 1.7 - 0.54 \log(PI) \tag{11.46}$$

PI = plasticity index

More recently, Morris and Williams (1994) gave the correlations of λ as

$$\lambda = 1.18e^{-0.08(PI)} + 0.57 \qquad (\text{for } PI > 5) \tag{11.47}$$

and

$$\lambda = 7.01e^{0.08(LL)} + 0.57 \qquad (\text{for } LL > 20) \tag{11.48}$$

where LL = liquid limit (%).

11.14 Other Methods for Determining Undrained Shear Strength

A modified form of the vane shear test apparatus is the *Torvane* (Figure 11.36), which is a handheld device with a calibrated spring. This instrument can be used for determining c_u for tube specimens collected from the field during soil exploration, and it can be used in the field. The Torvane is pushed into the soil and then rotated until the soil fails. The undrained shear strength can be read at the top of the calibrated dial.

Figure 11.37 shows a *pocket penetrometer,* which is pushed directly into the soil. The unconfined compression strength (q_u) is measured by a calibrated spring. This device can be used both in the laboratory and in the field.

11.15 Sensitivity and Thixotropy of Clay

For many naturally deposited clay soils, the unconfined compression strength is greatly reduced when the soils are tested after remolding without any change in

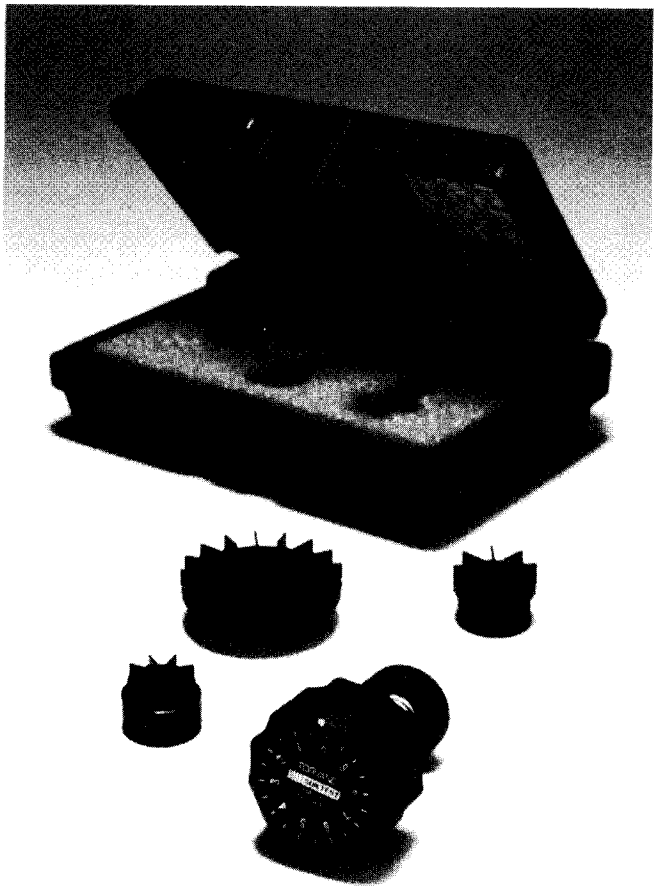

Figure 11.36
Torvane (courtesy of Soiltest, Inc., Lake Bluff, Illinois)

Figure 11.37
Pocket penetrometer (courtesy of Soiltest, Inc., Lake Bluff, Illinois)

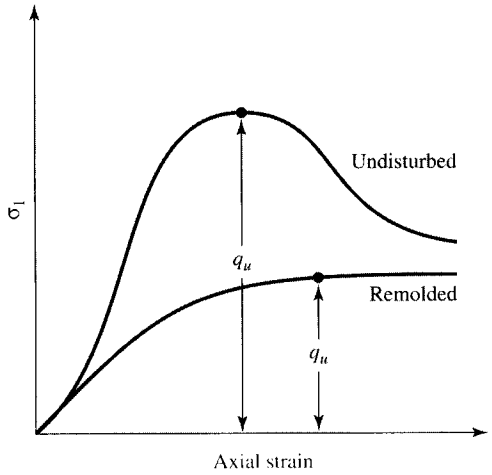

Figure 11.38 Unconfined compression strength for undisturbed and remolded clay

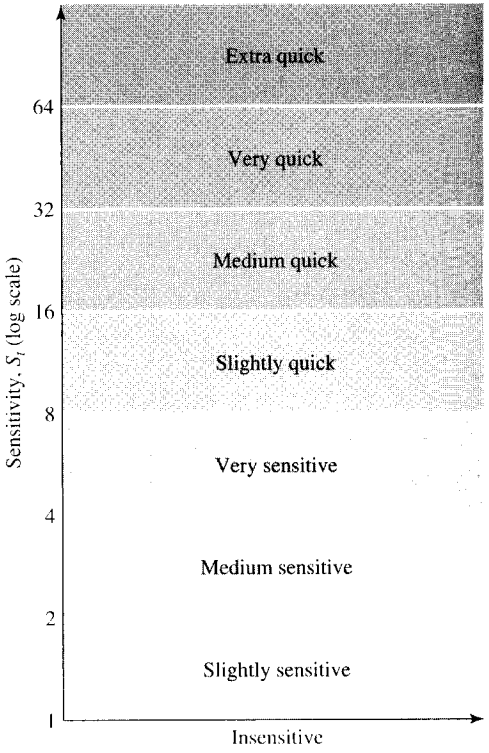

Figure 11.39 Classification of clays based on sensitivity

the moisture content, as shown in Figure 11.38. This property of clay soils is called *sensitivity*. The degree of sensitivity may be defined as the ratio of the unconfined compression strength in an undisturbed state to that in a remolded state, or

$$S_t = \frac{q_{u(\text{undisturbed})}}{q_{u(\text{remolded})}} \tag{11.49}$$

The sensitivity ratio of most clays ranges from about 1 to 8; however, highly flocculent marine clay deposits may have sensitivity ratios ranging from about 10 to 80. Some clays turn to viscous fluids upon remolding. These clays are found mostly in the previously glaciated areas of North America and Scandinavia. Such clays are referred to as *quick* clays. Rosenqvist (1953) classified clays on the basis of their sensitivity. This general classification is shown in Figure 11.39.

The loss of strength of clay soils from remolding is caused primarily by the destruction of the clay particle structure that was developed during the original process of sedimentation.

If, however, after remolding, a soil specimen is kept in an undisturbed state (that is, without any change in the moisture content), it will continue to gain strength with time. This phenomenon is referred to as *thixotropy.* Thixotropy is a time-dependent, reversible process in which materials under constant composition and volume soften when remolded. This loss of strength is gradually regained with time when the materials are allowed to rest. This phenomenon is illustrated in Figure 11.40a.

Most soils, however, are partially thixotropic — that is, part of the strength loss caused by remolding is never regained with time. The nature of the strength-time variation for partially thixotropic materials is shown in Figure 11.40b. For soils, the difference between the undisturbed strength and the strength after thixotropic hardening can be attributed to the destruction of the clay-particle structure that was developed during the original process of sedimentation.

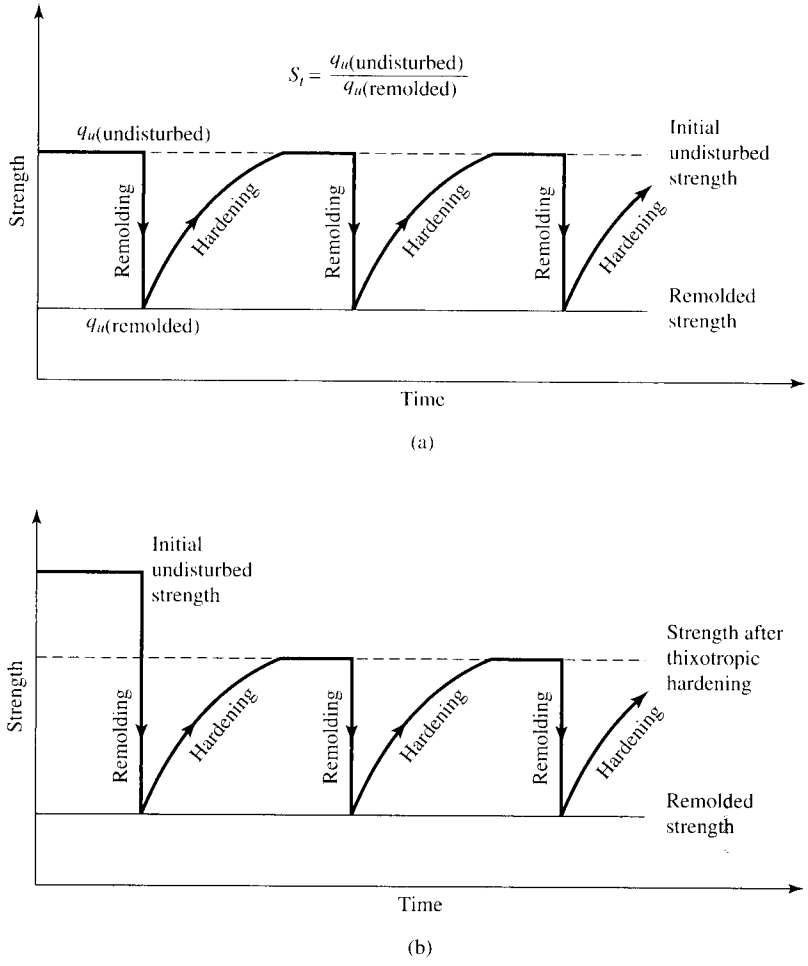

Figure 11.40 Behavior of (a) thixotropic material; (b) partially thixotropic material

Table 11.6 Empirical Equations Related to c_u and σ'_O

Reference	Relationship	Remarks
Skempton (1957)	$\frac{c_{u(\text{VST})}}{\sigma'_O} = 0.11 + 0.0037(PI)$ PI = plasticity index (%) $c_{u(\text{VST})}$ = undrained shear strength from vane shear test	For normally consolidated clay
Chandler (1988)	$\frac{c_{u(\text{VST})}}{\sigma'_c} = 0.11 + 0.0037(PI)$ σ'_c = preconsolidation pressure	Can be used in overconsolidated soil; accuracy ±25%; not valid for sensitive and fissured clays
Jamiolkowski et al. (1985)	$\frac{c_u}{\sigma'_c} = 0.23 \pm 0.04$	For lightly overconsolidated clays
Mesri (1989)	$\frac{c_u}{\sigma'_O} = 0.22$	
Ladd et al. (1977)	$\frac{\left(\frac{c_u}{\sigma'_O}\right)_{\text{overconsolidated}}}{\left(\frac{c_u}{\sigma'_O}\right)_{\text{normally consolidated}}} = (OCR)^{0.8}$ OCR = overconsolidation ratio	

11.16 Empirical Relationships between Undrained Cohesion (c_u) and Effective Overburden Pressure (σ'_O)

Several empirical relationships can be observed between c_u and the effective overburden pressure (σ'_O) in the field. Some of these relationships are summarized in Table 11.6.

The overconsolidation ratio was defined in Chapter 10 as

$$OCR = \frac{\sigma'_c}{\sigma'_O} \tag{11.50}$$

where σ'_c = preconsolidation pressure.

Example 10.8

A soil profile is shown in Figure 11.41. The clay is normally consolidated. Its liquid limit is 60 and its plastic limit is 25. Estimate the unconfined compression strength of the clay at a depth of 10 m measured from the ground surface. Use Skempton's relationship from Table 11.6 and Eqs. (11.45) and (11.46).

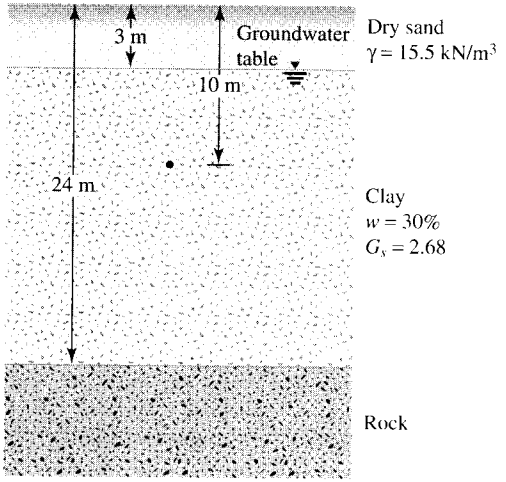

Figure 11.41

Solution

For the saturated clay layer, the void ratio is

$$e = wG_s = (2.68)(0.3) = 0.8$$

The effective unit weight is

$$\gamma'_{\text{clay}} = \left(\frac{G_s - 1}{1 + e}\right)\gamma_w = \frac{(2.68 - 1)(9.81)}{1 + 0.8} = 9.16 \text{ kN/m}^3$$

The effective stress at a depth of 10 m from the ground surface is

$$\sigma'_O = 3\gamma_{\text{sand}} + 7\gamma'_{\text{clay}} = (3)(15.5) + (7)(9.16)$$
$$= 110.62 \text{ kN/m}^2$$

From Table 11.6,

$$\frac{c_{u(\text{VST})}}{\sigma'_O} = 0.11 + 0.0037(PI)$$

$$\frac{c_{u(\text{VST})}}{110.62} = 0.11 + 0.0037(60 - 25)$$

and

$$c_{u(\text{VST})} = 26.49 \text{ kN/m}^2$$

From Eqs. (11.45) and (11.46), we get

$$c_u = \lambda c_{u(\text{VST})}$$
$$= [1.7 - 0.54 \log(PI)]c_{u(\text{VST})}$$
$$= [1.7 - 0.54 \log(60 - 25)]26.49 = 22.95 \text{ kN/m}^2$$

So the unconfined compression strength is

$$q_u = 2c_u = (2)(22.95) = \mathbf{45.9 \text{ kN/m}^2}$$

■

11.17 Shear Strength of Unsaturated Cohesive Soils

The equation relating total stress, effective stress, and pore water pressure for unsaturated soils, can be expressed as

$$\sigma' = \sigma - u_a + \chi(u_a - u_w) \tag{11.51}$$

where σ' = effective stress
σ = total stress
u_a = pore air pressure
u_w = pore water pressure

When the expression for σ' is substituted into the shear strength equation [Eq. (11.3)], which is based on effective stress parameters, we get

$$\tau_f = c' + [\sigma - u_a + \chi(u_a - u_w)]\tan \phi' \tag{11.52}$$

The values of χ depend primarily on the degree of saturation. With ordinary triaxial equipment used for laboratory testing, it is not possible to determine accurately the effective stresses in unsaturated soil specimens, so the common practice is to conduct undrained triaxial tests on unsaturated specimens and measure only the total stress. Figure 11.42 shows a total stress failure envelope obtained from a number of undrained triaxial tests conducted with a given initial degree of saturation. The failure envelope is generally curved. Higher confining pressure causes higher compression of the air in void spaces; thus, the solubility of void air in void water is increased. For design purposes, the curved envelope is sometimes approximated as a straight line, as shown in Figure 11.42, with an equation as follows:

$$\tau_f = c + \sigma \tan \phi \tag{11.53}$$

(Note that c and ϕ in the preceding equation are empirical constants.)

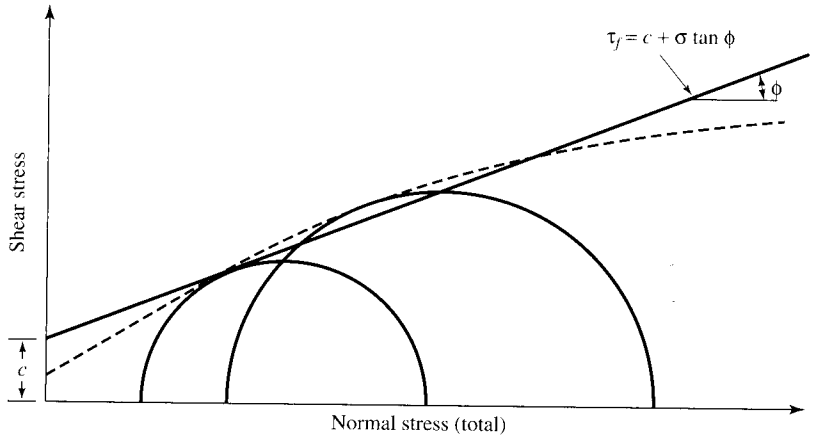

Figure 11.42 Total stress failure envelope for unsaturated cohesive soils

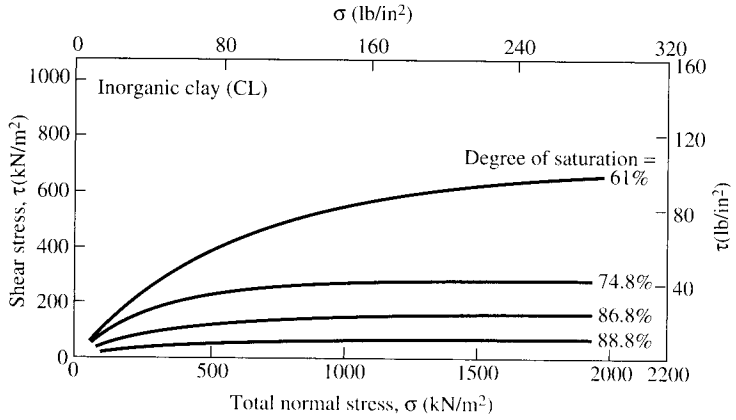

Figure 11.43 Variation of the total stress failure envelope with change of initial degree of saturation obtained from undrained tests of an inorganic clay (after Casagrande and Hirschfeld, 1960)

Figure 11.43 shows the variation of the total stress envelopes with change of the initial degree of saturation obtained from undrained tests on an inorganic clay. Note that for these tests the specimens were prepared with approximately the same initial dry unit weight of about 16.7 kN/m^3 (106 lb/m^3). For a given total normal stress, the shear stress needed to cause failure decreases as the degree of saturation increases. When the degree of saturation reaches 100%, the total stress failure envelope becomes a horizontal line that is the same as with the $\phi = 0$ concept.

In practical cases where a cohesive soil deposit may become saturated because of rainfall or a rise in the groundwater table, the strength of partially saturated clay should not be used for design considerations. Instead, the unsaturated soil specimens collected from the field must be saturated in the laboratory and the undrained strength determined.

11.18 Summary and General Comments

In this chapter, the shear strengths of grandular and cohesive soils were examined. Laboratory procedures for determining the shear strength parameters were described.

In textbooks, determination of the shear strength parameters of cohesive soils appears to be fairly simple. However, in practice, the proper choice of these parameters for design and stability checks of various earth, earth-retaining, and earth-supported structures is very difficult and requires experience and an appropriate theoretical background in geotechnical engineering. In this chapter, three types of strength parameters (*consolidated-drained, consolidated-undrained,* and *unconsolidated-undrained*) were introduced. Their use depends on drainage conditions.

Consolidated-drained strength parameters can be used to determine the long-term stability of structures such as earth embankments and cut slopes. Consolidated-undrained shear strength parameters can be used to study stability problems relating to cases where the soil initially is fully consolidated and then there is rapid loading.

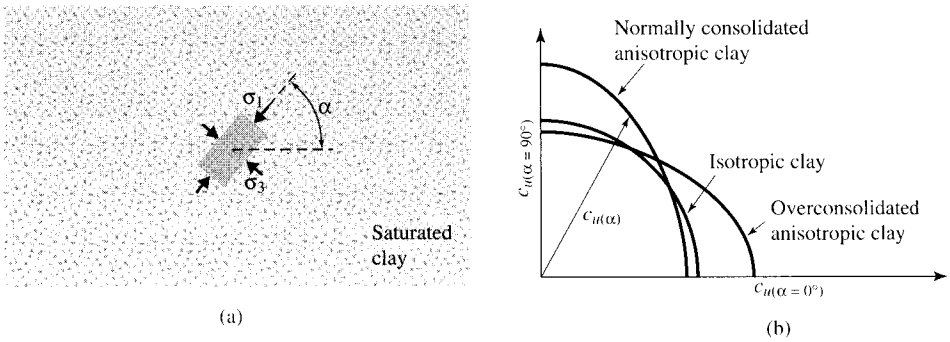

Figure 11.44 Strength anisotropy in clay

An excellent example of this is the stability of slopes of earth dams after rapid drawdown. The unconsolidated-undrained shear strength of clays can be used to evaluate the end-of-construction stability of saturated cohesive soils with the assumption that the load caused by construction has been applied rapidly and there has been little time for drainage to take place. The bearing capacity of foundations on soft saturated clays and the stability of the base of embankments on soft clays are examples of this condition.

The unconsolidated-undrained shear strength of some saturated clays can vary depending on the direction of load application; this is referred to as *anisotropy with respect to strength.* Anisotropy is primarily caused by the nature of the deposition of the cohesive soils, and subsequent consolidation makes the clay particles orient perpendicular to the direction of the major principal stress. Parallel orientation of the clay particles can cause the strength of clay to vary with direction. Figure 11.44a shows an element of saturated clay in a deposit with the major principal stress making an angle α with respect to the horizontal. For anisotropic clays, the magnitude of c_u will be a function of α. For normally consolidated clays, $c_{u(\alpha=90°)} > c_{u(\alpha=0°)}$; for overconsolidated clays, $c_{u(\alpha=90°)} < c_{u(\alpha=0°)}$. Figure 11.44b shows the directional variation for $c_{u(\alpha)}$. The anisotropy with respect to strength for clays can have an important effect on the load-bearing capacity of foundations and the stability of earth embankments because the direction of the major principal stress along the potential failure surfaces changes.

The sensitivity of clays was discussed in Section 11.15. It is imperative that sensitive clay deposits are properly identified. For instance, when machine foundations (which are subjected to vibratory loading) are constructed over sensitive clays, the clay may substantially lose its load-bearing capacity, and failure may occur.

Problems

11.1 A direct shear test was conducted on a specimen of dry sand with a normal stress of 200 kN/m^2. Failure occurred at a shear stress of 175 kN/m^2. The size of the specimen tested was 75 mm × 75 mm × 30 mm (height). Determine the angle of friction, ϕ'. For a normal stress of 150 kN/m^2, what shear force would be required to cause failure in the specimen?

11.2 The size of a sand specimen in a direct shear test was 50 mm × 50 mm × 30 mm (height). It is known that, for the sand, $\tan \phi' = 0.65/e$ (where e = void ratio) and the specific gravity of solids, $G_s = 2.68$. During the test a normal stress of 150 kN/m^2 was applied. Failure occurred at a shear stress of 110 kN/m^2. What was the mass of the sand specimen?

11.3 Following are the results of four drained direct shear tests on a normally consolidated clay:

Size of specimen = 60 mm × 60 mm
Height of specimen = 30 mm

Test no.	Normal force (N)	Shear force at failure (N)
1	200	155
2	300	230
3	400	310
4	500	385

Draw a graph for the shear stress at failure against the normal stress and determine the drained angle of friction (ϕ') from the graph.

11.4 Following are the results of four drained direct shear tests on a normally consolidated clay:

Specimen size: diameter of specimen = 2 in.
height of specimen = 1 in.

Test no.	Normal force (lb)	Shear force at failure (lb)
1	60	37.5
2	90	55
3	110	70
4	125	80

Draw a graph for shear stress at failure against the normal stress and determine the drained angle of friction (ϕ') from the graph.

11.5 The equation of the effective stress failure envelope for a loose sandy soil was obtained from a direct shear test as $\tau_f = \sigma' \tan 30°$. A drained triaxial test was conducted with the same soil at a chamber confining pressure of 10 lb/in.^{2}

a. Calculate the deviator stress at failure.

b. Estimate the angle that the failure plane makes with the major principal plane.

c. Determine the normal stress and shear stress (when the specimen failed) on a plane that makes an angle of 30° with the major principal plane. Also, explain why the specimen did not fail along the plane during the test.

11.6 The relationship between the relative density D_r and the angle of friction, ϕ', of a sand can be given as $\phi'^\circ = 28 + 0.18\, D_r$ (D_r is in %). A drained triaxial test on the same sand was conducted with a chamber confining pressure of 120 kN/m^2. The relative density of compaction was 65%. Calculate the major principal stress at failure.

11.7 For a normally consolidated clay, the results of a drained triaxial test are as follows:

Chamber confining pressure = 15 lb/in.^{2}
Deviator stress at failure = 34 lb/in.^{2}

Determine the soil friction angle, ϕ'.

11.8 For a normally consolidated clay, it is given that $\phi' = 24°$. In a drained triaxial test, the specimen failed at a deviator stress of 175 kN/m^2. What was the chamber confining pressure, σ_3'?

11.9 For a normally consolidated clay, it is given that $\phi' = 28°$. In a drained triaxial test, the specimen failed at a deviator stress at 30 lb/in.^{2} What was the chamber confining pressure, σ_3'?

11.10 A consolidated-drained triaxial test was conducted on a normally consolidated clay. The results were as follows:

$\sigma_3 = 250$ kN/m^2
$(\Delta\sigma_d)_f = 275$ kN/m^2

Determine the following:

a. Angle of friction, ϕ'
b. Angle θ that the failure plane makes with the major principal plane
c. Normal stress, σ', and shear stress, τ_f, on the failure plane

11.11 The results of two drained triaxial tests on a saturated clay are as follows:

Specimen I: chamber confining pressure = 70 kN/m^2
deviator stress at failure = 215 kN/m^2
Specimen II: chamber confining pressure = 120 kN/m^2
deviator stress at failure = 260 kN/m^2

Calculate the shear strength parameters of the soil.

11.12 If a specimen of clay described in Problem 11.11 is tested in a triaxial apparatus with a chamber confining pressure of 200 kN/m^2, what will be the major principal stress at failure? Assume full drained condition during the test.

11.13 A sandy soil has a drained angle of friction of 35°. In a drained triaxial test on the same soil, the deviator stress at failure is 2.69 ton/ft^2. What is the chamber confining pressure?

11.14 A deposit of sand is shown in Figure 11.45. Find the maximum shear resistance in kN/m^2 along a horizontal plane located 10 m below the ground surface.

11.15 A consolidated-undrained test on a normally consolidated clay yielded the following results:

$\sigma_3 = 15$ lb/in.^{2}
Deviator stress, $(\Delta\sigma_d)_f = 11$ lb/in.^{2}
Pore pressure, $(\Delta u_d)_f = 7.2$ lb/in.^{2}

Calculate the consolidated-undrained friction angle and the drained friction angle.

11.16 Repeat Problem 11.15, using the following values:

$\sigma_3 = 140$ kN/m^2
$(\Delta\sigma_d)_f = 125$ kN/m^2
$(\Delta u_d)_f = 75$ kN/m^2

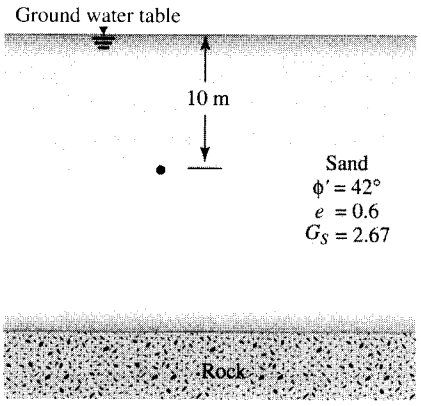

Figure 11.45

11.17 The shear strength of a normally consolidated clay can be given by the equation $\tau_f = \sigma' \tan 31°$. A consolidated-undrained test was conducted on the clay. Following are the results of the test:

Chamber confining pressure = 112 kN/m^2

Deviator stress at failure = 100 kN/m^2

Determine

a. The consolidated-undrained friction angle, ϕ

b. The pore water pressure developed in the clay specimen at failure

11.18 For the clay specimen described in Problem 11.17, what would have been the deviator stress at failure if a drained test would have been conducted with the same chamber confining pressure (i.e., $\sigma_3 = 112$ kN/m^2)?

11.19 A silty sand has a consolidated-undrained friction angle of 22° and a drained friction angle of 32° ($c' = 0$). If a consolidated-undrained test on such a soil is conducted at a chamber confining pressure of 1.2 ton/ft^2, what will be the major principal stress (total) at failure? Also, calculate the pore pressure that will be generated in the soil specimen at failure.

11.20 Repeat Problem 11.19, using the following values:

$\phi = 19°$

$\phi' = 28°$

$\sigma_3 = 85$ kN/m^2

11.21 The following are the results of a consolidated-undrained triaxial test in a clay:

Specimen no.	σ_3 (kN/m^2)	σ_1 at failure (kN/m^2)
I	192	375
II	384	636

Draw the total stress Mohr's circles and determine the shear strength parameters for consolidated undrained conditions (i.e., ϕ and c).

11.22 The consolidated-undrained test results of a saturated clay specimen are as follows:

$\sigma_3 = 97 \text{ kN/m}^2$

σ_1 at failure $= 197 \text{ kN/m}^2$

What will be the axial stress at failure if a similar specimen is subjected to an unconfined compression test?

11.23 The friction angle, ϕ', of a normally consolidated clay specimen collected during field exploration was determined from drained triaxial tests to be 25°. The unconfined compression strength, q_u, of a similar specimen was found to be 100 kN/m^2. Determine the pore water pressure at failure for the unconfined compression test.

11.24 Repeat Problem 11.23 using the following values:

$\phi' = 23°$

$q_u = 120 \text{ kN/m}^2$

11.25 The results of two consolidated-drained triaxial tests on a clayey soil are as follows:

Test no.	σ'_3 (lb/in.^{2})	$\sigma'_{1(\text{failure})}$ (lb/in.^{2})
1	27	73
2	12	48

Use the failure envelope equation given in Example 11.7—that is, $q' = m + p' \tan \alpha$. (Do not plot the graph.)

a. Find m and α.

b. Find c' and ϕ'.

11.26 A 15-m-thick normally consolidated clay layer is shown in Figure 11.46. The plasticity index of the clay is 18. Estimate the undrained cohesion as would be determined from a vane shear test at a depth of 6 m below the ground surface. Use Skempton's equation in Table 11.6.

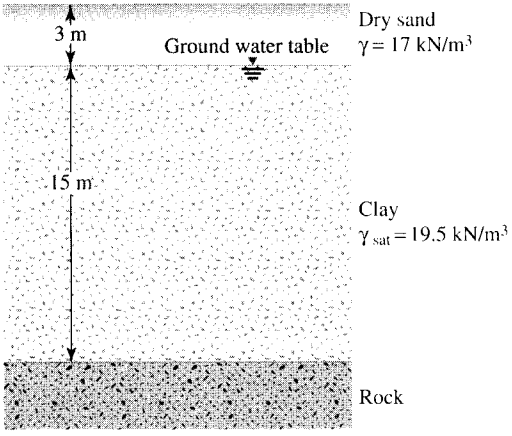

Figure 11.46

References

ACAR, Y. B., DURGUNOGLU, H. T., and TUMAY, M. T. (1982). "Interface Properties of Sand," *Journal of the Geotechnical Engineering Division,* ASCE, Vol. 108, No. GT4, 648–654.

AMERICAN SOCIETY FOR TESTING AND MATERIALS (1994). *Annual Book of ASTM Standards,* Vol. 04.08, Philadelphia, Pa.

BISHOP, A. W., and BJERRUM, L. (1960). "The Relevance of the Triaxial Test to the Solution of Stability Problems," *Proceedings,* Research Conference on Shear Strength of Cohesive Soils, ASCE, 437–501.

BJERRUM, L. (1974). "Problems of Soil Mechanics and Construction on Soft Clays," Norwegian Geotechnical Institute, *Publication No. 110,* Oslo.

BJERRUM, L., and SIMONS, N. E. (1960). "Compression of Shear Strength Characteristics of Normally Consolidated Clay," *Proceedings,* Research Conference on Shear Strength of Cohesive Soils, ASCE, 711–726.

BLACK, D. K., and LEE, K. L. (1973). "Saturating Laboratory Samples by Back Pressure," *Journal of the Soil Mechanics and Foundations Division,* ASCE, Vol. 99, No. SM1, 75–93.

CASAGRANDE, A., and HIRSCHFELD, R. C. (1960). "Stress Deformation and Strength Characteristics of a Clay Compacted to a Constant Dry Unit Weight," *Proceedings,* Research Conference on Shear Strength of Cohesive Soils, ASCE, 359–417.

CHANDLER, R. J. (1988). "The *in situ* Measurement of the Undrained Shear Strength of Clays Using the Field Vane," *STP 1014, Vane Shear Strength Testing in Soils: Field and Laboratory Studies,* ASTM, 13–44.

COULOMB, C. A. (1776). "Essai sur une application des regles de Maximums et Minimis á quelques Problèmes de Statique, relatifs á l'Architecture," *Memoires de Mathematique et de Physique,* Présentés, á l'Academie Royale des Sciences, Paris, Vol. 3, 38.

JAMIOLKOWSKI, M., LADD, C. C., GERMAINE, J. T., and LANCELLOTTA, R. (1985). "New Developments in Field and Laboratory Testing of Soils," *Proceedings,* XIth International Conference on Soil Mechanics and Foundation Engineering, San Francisco, Vol. 1, 57–153.

KENNEY, T. C. (1959). "Discussion," *Proceedings,* ASCE, Vol. 85, No. SM3, 67–79.

LADD, C. C., FOOTE, R., ISHIHARA, K., SCHLOSSER, F., and POULOS, H. G. (1977). "Stress Deformation and Strength Characteristics," *Proceedings,* 9th International Conference on Soil Mechanics and Foundation Engineering, Tokyo, Vol. 2, 421–494.

LAMBE, T. W. (1964). "Methods of Estimating Settlement," *Journal of the Soil Mechanics and Foundations Division,* ASCE, Vol. 90, No. SM5, 47–74.

MESRI, G. (1989). "A Re-evaluation of $s_{u(\text{mob})} \approx 0.22\,\sigma_p$ Using Laboratory Shear Tests," *Canadian Geotechnical Journal,* Vol. 26, No. 1, 162–164.

MOHR, O. (1900). "Welche Umstände Bedingen die Elastizitätsgrenze und den Bruch eines Materiales?" *Zeitschrift des Vereines Deutscher Ingenieure,* Vol. 44, 1524–1530, 1572–1577.

MORRIS, P. M., and WILLIAMS, D. J. (1994). "Effective Stress Vane Shear Strength Correction Factor Correlations," *Canadian Geotechnical Journal,* Vol. 31, No. 3, 335–342.

ROSENQVIST, I. TH. (1953). "Considerations on the Sensitivity of Norwegian Quick Clays," *Geotechnique,* Vol. 3, No. 5, 195–200.

SKEMPTON, A. W. (1954). "The Pore Water Coefficients *A* and *B*," *Geotechnique,* Vol. 4, 143–147.

SKEMPTON, A. W. (1957). "Discussion: The Planning and Design of New Hong Kong Airport," *Proceedings,* Institute of Civil Engineers, London, Vol. 7, 305–307.

SKEMPTON, A. W. (1964). "Long-Term Stability of Clay Slopes," *Geotechnique,* Vol. 14, 77.